Nucleic Acids Research, 2024, **52**, 10965–10985
https://doi.org/10.1093/nar/gkae705
Advance access publication date: 16 August 2024
Genome integrity, repair and replication

Loss of DNA glycosylases improves health and cognitive function in a *C. elegans* model of human tauopathy

Vinod Tiwari [1], Elisabeth Buvarp [1], Fivos Borbolis [2], Chandrakala Puligilla [3], Deborah L. Croteau [1,4], Konstantinos Palikaras [2,*] and Vilhelm A. Bohr [1,5,*]

[1]Section on DNA Repair, National Institute on Aging, Baltimore, MD 21224, USA
[2]Department of Physiology, Medical School, National and Kapodistrian University of Athens, Athens, 11527, Greece
[3]Section for Telomere Maintenance, LGG, National Institute on Aging, Baltimore, MD 21224, USA
[4]Computational Biology & Genomics Core, LGG, NIA, Baltimore, MD 21224, USA
[5]Center for Healthy Aging, University of Copenhagen, 2200 N, Denmark

[*]To whom correspondence should be addressed. Tel: +45 35 32 67 98; Email: vbohr@sund.ku.dk
Correspondence may also be addressed to Konstantinos Palikaras. Tel: +30 2107462552; Email: palikarask@med.uoa.gr
Present address: Vinod Tiwari, Department of Diabetes & Cancer Metabolism, Beckman Research Institute of City of Hope, Duarte, CA 91010, USA.

Abstract

Alzheimer's disease (AD) is a neurodegenerative disorder representing a major burden on families and society. Some of the main pathological hallmarks of AD are the accumulation of amyloid plaques (Aβ) and tau neurofibrillary tangles. However, it is still unclear how Aβ and tau aggregates promote specific phenotypic outcomes and lead to excessive oxidative DNA damage, neuronal cell death and eventually to loss of memory. Here we utilized a *Caenorhabditis elegans (C. elegans)* model of human tauopathy to investigate the role of DNA glycosylases in disease development and progression. Transgenic nematodes expressing a pro-aggregate form of tau displayed altered mitochondrial content, decreased lifespan, and cognitive dysfunction. Genetic ablation of either of the two DNA glycosylases found in *C. elegans*, NTH-1 and UNG-1, improved mitochondrial function, lifespan, and memory impairment. NTH-1 depletion resulted in a dramatic increase of differentially expressed genes, which was not apparent in UNG-1 deficient nematodes. Our findings clearly show that in addition to its enzymatic activity, NTH-1 has non-canonical functions highlighting its modulation as a potential therapeutic intervention to tackle tau-mediated pathology.

Graphical abstract

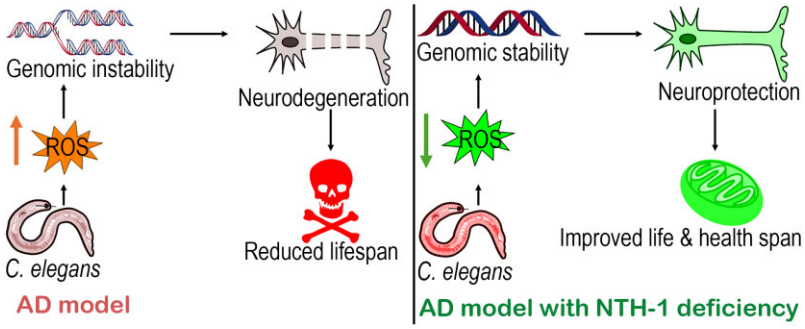

Introduction

Alzheimer's disease (AD) is a progressive neurological disorder, characterized by Aβ plaques and neurofibrillary tau tangle formation (1). The loss of synapses and synaptic plasticity in AD is directly related to cognitive decline. The major risk factors associated with AD include aging, genomic stress, and mitochondrial dysfunction (1–3). The post mitotic neuronal cells are more sensitive to oxidative stress, which is induced by the elevated production of reactive oxygen species (ROS) (2). Age-related oxidative stress exhibits a proportional increase and is concomitant with mitochondrial impairments. Notably, the brain affected by AD also manifests increased levels of ROS, which actively contributes to the pathophysiology of AD (2,4). Recently, it was demonstrated that the disruption of genome organization and stability by persistent DNA double-strand breaks promotes the progression of neurodegenerative diseases (5). However, the exact cause of age-associated genomic stress in AD remains elusive.

Base excision repair (BER) is a major DNA repair pathway, which alleviates both endogenous and exogenous oxidative DNA damage. The BER pathway is critical for genome stability and human health. It is initiated by the recognition and removal of the damaged DNA base by a DNA glycosylase. This is followed by incision of the abasic site, replacement and/or synthesis of the missing nucleotide(s), end processing, and finally ligation of the nick (6). Previously, it was shown by us, and others, that there are significant BER deficiencies in AD patients due to limited DNA base damage

Received: June 22, 2023. **Revised:** July 20, 2024. **Editorial Decision:** July 26, 2024. **Accepted:** August 11, 2024
Published by Oxford University Press on behalf of Nucleic Acids Research 2024.

processing by DNA glycosylases and reduced DNA synthesis capacity by DNA polymerase β (7–9). Additionally, deficiency of DNA polymerase β, a crucial enzyme in the base excision repair (BER) pathway, not only leads to neurodegeneration, but also exacerbates AD pathological features (10). Thus, deficiencies in BER pathway proteins may worsen the AD pathology. On the contrary, several reports suggest a potential beneficial impact of BER pathway deficits. Indeed, a study revealed that mice deficient in alkyladenine-DNA glycosylase (AAG) were protected from alkylating agent-induced DNA damage (11). Further supporting this notion, a recent study by SenGupta et al. using *C. elegans* demonstrated that deficiency of NTH-1 promotes neuroprotection in a nematode model of Parkinson's disease (12). Consequently, understanding the role of BER imbalance on neurological function and animal behaviour presents a challenging and important task.

C. elegans, a simple model organism, is extensively utilized in studies that focus on DNA damage response, human aging, and pathological conditions such as neurodegenerative disorders (13). Several biological processes, including development, neuronal function, behaviour, and aging, exhibit similarities between humans and nematodes (14). In the context of Alzheimer's disease (AD) research, *C. elegans* models have been widely employed due to their ability to mimic the memory loss observed in human patients (15). The short lifespan and well-defined physiology of *C. elegans* facilitates it as a versatile model system for investigating lifespan, cognitive function, and mitochondrial metabolism (13,14). Notably, the *C. elegans* genome encodes only two DNA glycosylases, in contrast to mammalian cells which have 11 DNA glycosylases (12). Consequently, *C. elegans* serves as a suitable model for investigating the impact of DNA glycosylase deficiencies in a tauopathy nematode model. The two glycosylases in *C. elegans* are UNG-1 and NTH-1. UNG-1 is a monofunctional DNA glycosylase while NTH-1 is a bifunctional DNA glycosylase, which excises oxidized DNA bases and incises the DNA phosphodiester backbone 3′ to the AP site. It is worth noting that NTH-1 is located in both the nucleus and mitochondria. NTH-1 deficient animals display normal life span, embryonic viability, and brood size (16–18).

Here, we investigated the role of DNA glycosylases on lifespan and health span in a tauopathy *C. elegans* model. We demonstrate that incomplete repair and gradual accumulation of endogenous DNA base damage through DNA glycosylase initiated BER, generates genomic stress during aging. The observed improvements in AD pathological features and enhanced mitochondrial activity in DNA glycosylase deficient nematodes suggest that BER imbalance may exert modulatory effects on neurodegeneration and AD pathophysiology.

Materials and methods

C. elegans strains

Standard *C. elegans* strain maintenance procedures were followed. The nematode rearing temperature was 22°C for UNG-1 strains and 20°C for NTH-1 related strains based on our previous experiences with these models (19). The following strains were used in this study: N2: wild-type Bristol isolate (herein called 'N2'), GRU102: *gnaIs2* [$p_{myo\text{-}2}$YFP; $p_{unc\text{-}119}$Abeta$_{1\text{-}42}$], *nth-1(ok724);* *gnaIs2* [$p_{myo\text{-}2}$YFP; $p_{unc\text{-}119}$Abeta$_{1\text{-}42}$], EVL1372: *lhIs84* [$p_{rgef\text{-}1}$3POTau::GFP], *nth-1(ok724)*; *lhIs84* [$p_{rgef\text{-}1}$3POTau::GFP], *ung-1(ok3593);* *lhIs84* [$p_{rgef\text{-}1}$3POTau::GFP], PHX10: N2; Ex10[$p_{myo\text{-}3}$UNG-1::mCherry; pRF4], BR5270: *byIs161*[$p_{rab\text{-}3}$F3ΔK280*;* $p_{myo\text{-}2}$mCherry] (herein called 'BR5270'), BR5271: *byIs162*[$p_{rab\text{-}3}$F3ΔK280(I277P)(I308P*);* $p_{myo\text{-}2}$mCherry] (herein called 'BR5271'), RB2581: *ung-1(ok3593)III* (herein called 'UNG-1'), RB877: *nth-1(ok724)III* (herein called 'NTH-1'). Strains BR5270, BR5271, UNG-1 and NTH-1 were outcrossed for 6 generations into N2. Further, the outcrossed BR5270, BR5271 strains were crossed with UNG-1 and NTH-1 to get homozygote UNG-1;BR5270, UNG-1; BR5271, NTH-1;BR5270 and NTH-1;BR5271. These strains were maintained in 35-mm Petri dishes with NGM-agar seeded with *Escherichia coli* OP50 (an uracil-requiring mutant).

C. elegans brood size and embryonic viability assays

Individual late L4 staged worms were incubated in six separate OP50 seeded NGM plates at 20, or 22°C overnight. The next day, the worms were removed, and the number of eggs laid were counted. Then, 24h later the number of unhatched eggs were counted to access viability of these eggs.

Locomotion assays

10–15ul of M9 buffer were pipetted onto a glass slide, and individual worms were picked into the M9. Body bends were counted for 20s, with a complete left-right motion constituting each body bend. 10 worms were assayed per strain, and body bends for each worm were counted twice and averaged.

In order to get in-depth understanding of locomotion defect, NTH1-related worm locomotion was recorded by the Wormlab software (MBF Bioscience) on OP50 seeded NGM plate and captured at 15 frames per second rate. Synchronized day 1 worms were recorded for 1min and the per frame movement data was exported to excel and movement velocity was evaluated by measuring the distance each worm moved and graph was plotted using GraphPad Prism software.

Memory assays

Chemotaxis to volatile compounds was performed at room temperature, on 9cm agar plates as described previously (20). The chemotaxis index was calculated by subtracting the number of animals found at the trap from the number of animals at the source of the chemical, divided by the total number of animals subjected to the assay (20). The resulting values were expressed as percentiles. For conditioning to isoamyl alcohol, a droplet of 5µl isoamyl alcohol was placed on the lid of a conditioning non-bacterial seeded nematode growth medium plate. Animals were conditioned to isoamyl alcohol for 90 min. Both naïve and conditioned animals were exposed for 90min to isoamyl alcohol (IAA) (gradient sources: isoamyl alcohol, 1:100 dilution in water). One-day-old and three-day-old adult hermaphrodites were used in the behavioural assays. 3–4 biological experiments, with 100–300 adults (for each strain) were scored per assay.

C. elegans lifespan assays

Lifespan assays were conducted at either 22°C (UNG-1 set) or 20°C (NTH-1 set). A total of 100 worms were counted every day and transferred to freshly seeded NGM-OP50 plates for 1

week, then every other day after that. Worms that desiccated on the side of the plate, bagged from internal hatching, had vulvar ruptures, or were otherwise missing were censored. For each lifespan assay, 100 worms per condition were divided evenly among five plates (≥20 worms/plate) unless otherwise noted. Lifespan was analysed and graphed using a Kaplan-Meier plot in GraphPad prism.

For lifespan assays with treatments, drugs were prepared fresh and applied in small volumes (100μl) to achieve indicated concentration with respect to total media volume. Plates were overlaid with desired drug solution concentrations and allowed to reach equilibrium with total media for 30min–1h. For menadione, worms were transferred to fresh drug-equilibrated plates daily until their death. For cisplatin treatment, L4 stage worms were treated with cisplatin for 24h and then worms were transferred to fresh plates daily till the end of their life span. Menadione (1mM) and cisplatin (60μg/ml) concentrations were selected based on previously reported assays (21,22). In UV treatments, synchronized late L4 stage *C. elegans* strains worms were subjected to 75J/m^2 dose UVC on unseeded 35mm plate and were transferred to seeded plates after UVC treatment and scored, as described above.

RNA isolation and RNAseq data analysis

Each synchronized strain of *C. elegans* was grown on three 35mm NGM plates and harvested together as single datapoint for RNA isolation at day 1 stage of the life cycle. Worms were collected from plates and washed with M9 buffer 5 times through gravity. Approximately, 5000 worms per genotype were collected. Total RNA was extracted using RNeasy RNA extraction kits (Qiagen) and RNA integrity was measured by the RNA Nano 6000 Assay Kit of the Bioanalyzer 2100 system (Agilent Technologies, CA, USA). cDNA library fragments were purified with AMPure XP system (Beckman Coulter, Beverly, USA) and quality was assessed on the Agilent Bioanalyzer 2100 system. The clustering of the samples was performed on a cBot Cluster Generation System using TruSeq PE Cluster Kit v3-cBot-HS (Illumia) according to the manufacturer's instructions. The library preparations were sequenced on an Illumina Novaseq platform and 150 bp paired-end reads were generated. RNAseq reads were mapped to the *C. elegans* genome (WBcel235, Ensembl annotation) using HISAT2 (23). Raw read counts were normalized and subjected to differential expression analysis using the EdgeR library by Novogene, USA. The statistical model used to calculate *P*-values employed the negative binomial distribution method and the Benjamini-Hochberg multiple hypothesis test corrections was used to obtain false discovery rates. Differentially expressed genes were determined by comparison to each glycosylase cohort's N2 control worms, since the glycosylase strains were cultured differently. The set of significantly differentially expressed genes were those which had counts ≥100, an absolute value $\log_2$ fold-change ≥1 and adj-*P*-value ≤0.05. The collected genes were subjected to enrichment analysis using the site at Wormbase, https://wormbase.org/tools/enrichment/tea/tea.cgi/ (24,25).

Real-time quantitative PCR

Total RNA was prepared from frozen worm pellets of the indicated genetic background, using Nucleozol (Macherey-Nagel). Three populations of 150–200 worms were harvested at day 1 of adulthood and analysed independently in each experiment. Quality and quantity of RNA samples were determined using BioTek Cytation 5 reader (Agilent). Reverse transcription was carried out with iScipt RT cDNA Synthesis KIT (Bio-Rad) and quantitative PCR was performed using KAPA SYBR FAST Universal Kit (Kapa Biosystems) in the QuantStudio 5 Real-Time PCR system (Applied Biosystems). Relative amounts of mRNA were determined using the comparative Ct method for quantification and each sample was independently normalized to its endogenous reference gene (*ama-1*). Gene expression data are presented as the mean fold change ± SEM of all biological replicates relative to the indicated control. Statistical analysis was performed as indicated on each occasion. Primer sequences used for qRT-PCR are as follows: ama-1_FW: 5′-GCTATGGTGCCGAGACAAC-3′ / ama-1_RV: 5′-CCAGGAATGATAAGCGAGAAGAC-3′, rmh-2_FW: 5′-TCAAAAGAAACAATGCCCACCTTC-3′ / rmh-2_RV: 5′-CGATTGGTCATTCGCCGATTC-3′, cin-4_FW: 5′-CTTCCAAGCTGAAGGGCATC-3′ / cin-4_RV: 5′-GCACTATCGGCGATTTGATTCAC-3′, rfs-1_FW: 5′-GAGCTTCAGGATTCTTTAACTCG-3′, rfs-1_RV: 5′-CCACGCCAGTGTGTAATGTG-3′, NTH-1_FW: 5′-CTAATCGACTCGGCTGGATC-3′ / NTH-1_RV: 5′-GAAGTCTCTTCAGTCTCGCTC-3′, UNG-1_FW: 5′-GGGAGGATTTGCTCATAAGAAGG-3′ / UNG-1_RV: 5′-TCGGGTTTCGACCGGAATTTTC-3′.

Comparison with human and mouse data from Grubman *et al.* (26) and *Ali et al.* (27)

Gene set enrichment analysis pathways from BR5270 versus N2 were compared with pathways from single cell gene set enrichment analysis from the human entorhinal cortex AD versus control samples (from Figure 1 (26)). Out of the 314-consensus set of DE genes in BR5270, 305 could be mapped to the human and mouse genomes using Wormbase tool (https://wormbase.org//tools/mine/simplemine.cgi) and Biomart (biomart.genenames.org). Differential gene expression results between human AD and controls were obtained from pooling the single cell data from all cells from Grubman *et al.* (26). Grubman defined DE genes as having an FDR <0.01 and absolute log fold change greater than 0.5. We defined DE genes as stated above. The DE gene list from Ali et al. was derived from Ali *et al* (27) Supplementary Table S1 clusters and marker genes of Tg2576 Ad mice versus controls and based on an FDR <0.05 and $\log_2$ fold-change of |0.5|.

Immunohistochemistry and TUNEL assay

Day 1 synchronized strains of *C. elegans* were washed with M9 buffer followed by milliQ water twice. Animals were fixed on polylysin-coated slides (Thermo Scientific), and freeze cracked using a coverslip on dry ice block. Worm slides were fixed in acetone and methanol in 1:1 ratio for 10min at − 20°C, washed in PBS-T (1 × PBS, 0.1% Tween-20) for 5 min, followed by 30min blocking in PBS-TB (1 × PBS, 0.1% Tween-20, 0.5% BSA). For 8-oxo-dG staining, slides were incubated with 8-oxo-dG antibody (1:200) overnight at 4°C. The next day slides were washed three times for 10min in PBS-T and then incubated with the secondary antibody (Alexa Fluor 555-conjugated anti-mouse; 1:1500) at room temperature for 2h. Slides were mounted with prolong gold with DAPI. For TUNEL assay, fixed worm slides were permeabilized by proteinase K from the kit, followed by TdT and click-iT reaction as instructed in the user guide. Click-iT® Plus TUNEL Assay kit (Invitrogen) was used to perform TUNEL assay. Slides

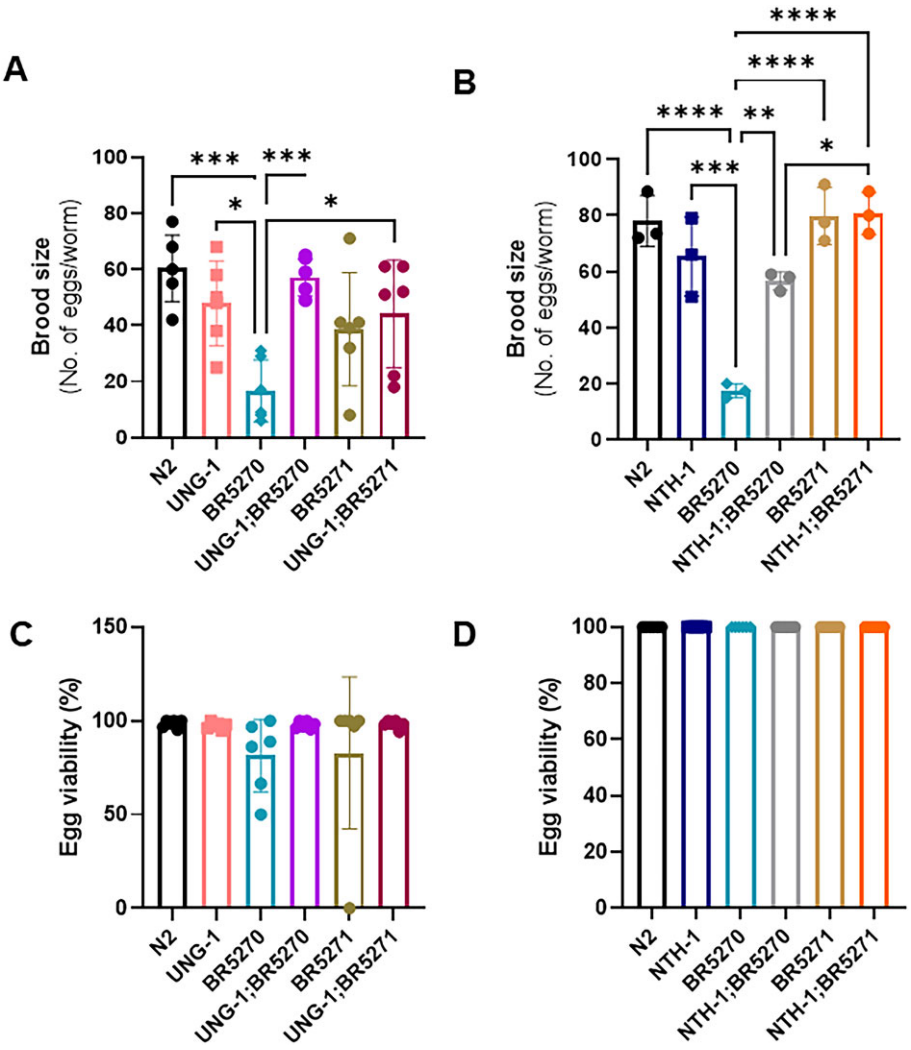

Figure 1. Loss of DNA glycosylases rescues brood size deficiency in AD worm. Brood size of day 1 adult worm (**A**) wild type (N2), UNG-1, BR5270, UNG-1;BR5270, BR5271 and UNG-1;BR5271 and (**B**) N2, NTH-1, BR5270, NTH-1;BR5270, BR5271 and NTH-1;BR5271 ($n = 3$–5 worms for each replicate). Egg viability was measured 24h after brood size in (**C**) N2, UNG-1, BR5270, UNG-1;BR5270, BR5271 and UNG-1;BR5271 and (**D**) N2, NTH-1, BR5270, NTH-1;BR5270, BR5271 and NTH-1;BR5271 worms. Brood size and viability statistical analyses were performed by one-way ANOVA followed by Tukey's multiple comparison test. Data showing ± SEM, $*P \leq 0.05$, $**P \leq 0.01$, $***P \leq 0.001$ and $****P \leq 0.0001$. Three biological replicates were performed.

were observed by Zeiss 980 LSM with Airyscan 2 confocal microscope and analysed for fluorescence.

Mitochondrial potential staining

Worms were incubated on OP50 seeded NGM plates with 200nM tetramethylrhodamine ethyl ester (TMRE) overnight. After overnight staining, the animals were washed with M9 buffer and transferred into a fresh NGM-OP50 plate for 90 min. Thereafter, worms were washed 3–5 times with M9 buffer to remove residual bacteria and placed into an unseeded plate. Worms were picked onto glass slides with a 3–5% agarose pad and immobilized by 50mM levamisole before mounting. Glass slides were observed by Zeiss 980 LSM with Airyscan 2 confocal microscope and analysed for fluorescence. As BR5270 and BR5271 have mCherry expression in the head region and have overlapping fluorescence with TMRE, the lower part of the worm body (below vulva) was scored for TMRE intensity in all strains, to remain consistent.

Statistical analysis

All statistical analyses were performed in GraphPad prism software as indicated. Brood size and viability statistical analyses were performed by one-way ANOVA followed by Tukey's multiple comparison test. Lifespan statistical analyses were performed on Kaplan–Meier survival curves by Log-rank (Mantel–Cox) tests (Supplementary Table S1). Chemotaxis data was analysed by two-way ANOVA followed by Tukey's multiple comparison test. Unpaired *t*-test was used to analyse 8-oxo-dG foci and TUNEL positive cells.

Results

Loss of DNA glycosylases improves brood size and lifespan of the tauopathy nematode model

DNA glycosylases play important roles in cell biology. Since *C. elegans* only has two glycosylases, NTH-1 and UNG-1, we examined their importance on tau-related pathology. While Aβ pathology precedes tau, it is currently appreciated that

tau deregulation is the driving force of cognitive dysfunction (28,29). Thus, understanding how DNA glycosylases are associated with tau-related pathology is particularly important. To examine the role of BER DNA glycosylases on tau-pathology, we utilized the tauopathy worm models BR5270 and BR5271, which pan-neuronally express the tau-aggregate F3ΔK280 and the anti-tau-aggregate fragments respectively, and thus BR5270 is the AD model and BR5271 its control (30). We first checked brood size and egg viability of the DNA glycosylase deficient worms. BR5270 nematodes displayed reduced brood size, and both UNG-1 and NTH-1 depletion rescued this defect (Figure 1A and B). Moreover, BR5270 animals displayed a delayed development compared to UNG-1 or NTH-1 deficient BR5270 nematodes. Notably, we did not detect any alteration in the brood size of BR5271, UNG-1 or NTH-1 deficient nematodes as compared to wild type (N2) animals (Figure 1A and B). Finally, we did not observe any defects in embryo viability (Figure 1C and D).

Lifespan assays were conducted to evaluate the effect of DNA glycosylase ablation on organismal physiology, AD features and survival (Figure 2 and Supplementary Table S1). We did not observe any differences in the median or maximum lifespan of UNG-1 (median lifespan 14 days) and/or NTH-1 deficient nematodes (median lifespan 20 days) compared to their wild type counterparts (14 and 20 days respectively) (Figure 2A–D and Supplementary Table S1). However, we observed reduced lifespan of BR5270 worms (median lifespan 10 for UNG-1 set and 15 days for NTH-1 set) (Figure 2G and H). Previous studies have shown that tau-expressing worms (BR5270) display impaired energy metabolism, reduced lifespan, and cognitive dysfunction (30,31). Interestingly, genetic ablation of UNG-1 or NTH-1 significantly improved the lifespan of tau-expressing nematodes (median lifespan 12 for UNG-1 set and 19 days for NTH-1 set) (Figure 2G and H). Taken together, our results suggest that both UNG-1 and NTH-1 DNA glycosylases contribute to tau-induced neurotoxicity affecting development and lifespan.

Loss of DNA glycosylases improves neuroplasticity in the tauopathy model

To assess whether loss of DNA glycosylases affect motor neuron activity, we first examined the locomotion rate in the respective genetic backgrounds (Figure 3A and B). Notably, neither UNG-1 nor NTH-1 depletion affected locomotion (Figure 3A and B). Moreover, tau-expressing nematodes displayed unaltered locomotion even upon UNG-1 and NTH-1 genetic ablation (Figure 3A and B). These results indicate that these animals do not have any intrinsic movement defects and can be used for chemotaxis assay to check their neuroplasticity.

Gradual cognitive and olfactory dysfunction are features seen in AD patients (32–34). Thus, we used an aversive olfactory learning chemotaxis assay to assess memory performance in the nematode model of tauopathy. In naïve conditions, worms move towards the taste cue (isoamyl alcohol - IAA) and we then associated this taste cue with starvation (35). If the worms have good memory, they avoid this cue and show a negative chemotaxis index as observed in the case of wild type (N2) animals (Figure 3C and D). Neither UNG-1 nor NTH-1 deficient worms presented any memory defect. On the contrary, the tau-expressing BR5270 nematodes displayed severe cognitive impairment, as has already been demonstrated (31). Interestingly, memory loss was improved upon UNG-1 or NTH-1 depletion in the tau-expressing worms (UNG-1;BR5270 and NTH-1;BR5270; Figure 3C and D). Notably, wild type (N2) and DNA glycosylases depleted animals that express an anti-aggregation fragment of tau (BR5271), do not display any locomotion or cognition defects (Figure 3C and D).

To investigate the potential influence of DNA glycosylases on tau aggregation further, we have utilized a recently developed nematode model expressing the aggregation-prone Tau(3PO) variant fused with GFP under the pan-neuronal promoter *rgef-1* (36). Interestingly, both NTH-1 and UNG-1 deficiency do not modify the rate of Tau(3PO) aggregate formation in young (day 1) animals but increase Tau(3PO)::GFP aggregates in old (day 5 and day 8) nematodes (Figure 4A and B). However, it significantly improves their locomotion defect (Figure 4C). These observations are in agreement with theories suggesting a protective role for the formation of aggregates but could also indicate that DNA glycosylases deficiency protects form tau-induced pathological phenotypes by ameliorating toxic effects that occur downstream of aggregation, or through the induction of independent compensatory mechanisms. Moreover, we examined the impact of DNA glycosylase deficiency on another Alzheimer's disease nematode model that expresses Aβ1–42 under the pan-neuronal promoter *unc-119* (37). Our findings indicate that the depletion of NTH-1 improves the impaired locomotion rate of 3-day-old nematodes expressing Aβ1–42 (Supplementary Figure S1). Recently, we have demonstrated that NTH-1 deficiency enhances the survival of dopaminergic neurons in a Parkinson's disease nematode model (12). Collectively, these results underscore the broad neuroprotective impact of inhibiting DNA glycosylase activity against proteotoxicity.

Loss of DNA glycosylases differentially regulates many genes in tau-expressing worms

To elucidate molecular mechanisms that may underly the neuroprotection and memory improvement in the context of tau pathology, we performed RNA sequencing (RNAseq) analysis to investigate the impact of DNA glycosylase depletion on gene expression (Figure 5 and Supplementary Figure S2). First, we show the loss of mRNA expression of the glycosylases in the various strains, as determined by both RNAseq and qRT-PCR (Figure 5A and Supplementary Figure S3A and B). Since the two glycosylase mutant strains were examined under slightly different temperature conditions, see Methods, for all subsequent analyses involving an N2, we compared each genotype to its respective wild type (N2u or N2n) strain to determine the level of gene expression changes. Note, the two N2 strains were originally derived from the same stock. Nonetheless, to remove genes that were changed due to differences in the N2 backgrounds, any gene with more than two-fold difference between the two N2 strains (N2u versus N2n) were removed from any comparisons to either N2, (276 DE genes between them, Supplementary Table S2). DE genes were defined as those with a $\log_2$ fold-change absolute value ≥ 1 and an adj-*P*-value ≤ 0.05.

A summary of each pairwise comparison and the DE genes that were up or down regulated is shown in Supplementary Table S2. At a basal level, NTH-1 knockout worms had dramatically more DE genes (44 genes for UNG1 worms (UNG-1_N2) compared to 2817 genes NTH1_N2 (Supplementary Table S2)). Each glycosylase's DE gene list was submitted to

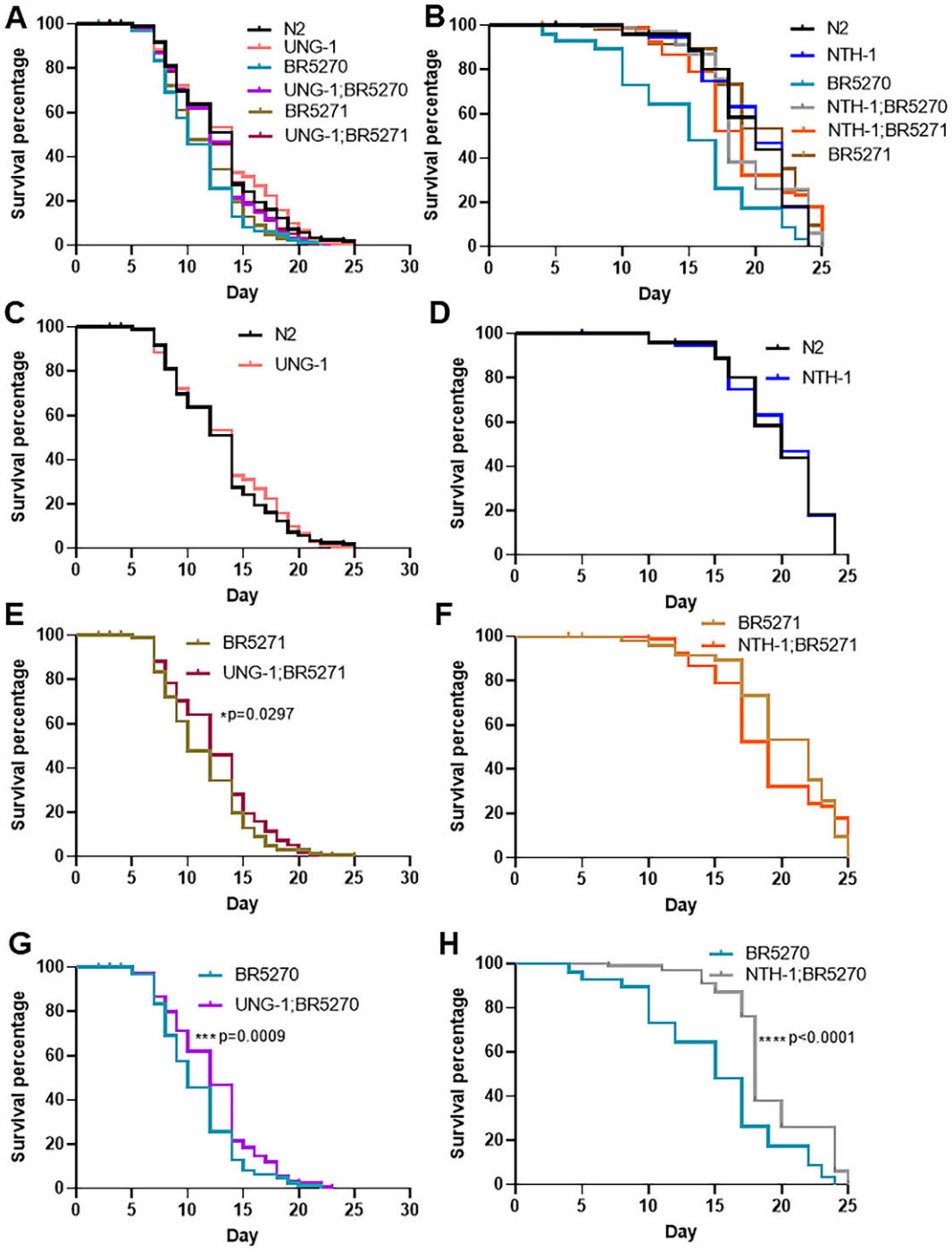

Figure 2. Loss of DNA glycosylases improves lifespan in tau-aggregation expressing worms. Lifespan of (**A**) all strains under UNG-1 deficiency, (**B**) all strains under NTH-1 deficiency, (**C**) wild type (N2) and UNG-1 strains, (**D**) N2 and NTH-1 strains, (**E**) BR5271 and UNG-1;BR5271 worms, (**F**) BR5271 and NTH-1;BR5271 worms, (**G**) BR5270 and UNG-1;BR5270 worms, (**H**) BR5270 and NTH-1;BR5270. Statistical analysis was performed on Kaplan-Meier survival curves by Logrank (Mantel–Cox) tests (see Supplementary Table S1 for detailed *P*-value) $*P \leq 0.05$, $**P \leq 0.01$, $***P \leq 0.001$ and $****P \leq 0.0001$ ($n = 20$ worms/study; total of 100 worms).

Wormbase enrichment analysis (24,25). Gene ontology terms were considered significant if they had a q-value ≤ 0.1. Due to the short list of genes for the UNG1 versus N2, no terms were found to be enriched. In contrast, 63 terms were enriched in the NTH1 versus N2 comparison and Supplementary Table S3 shows the full list of terms enriched in NTH-1 deficient worms. Figure 5B shows the top 15 terms. Among the top terms there were: DNA-directed RNA polymerase, splicing, actin terms, and several terms related to muscle.

Because the worm's behaviour is always compared mutant to N2, we conducted an analysis to identify a consensus set of genes consistently changed with tau-pathology relative to N2. First, the two BR5270 versus their respective N2 DE gene lists (NTH-1 set and UNG-1 set) were compared to the two

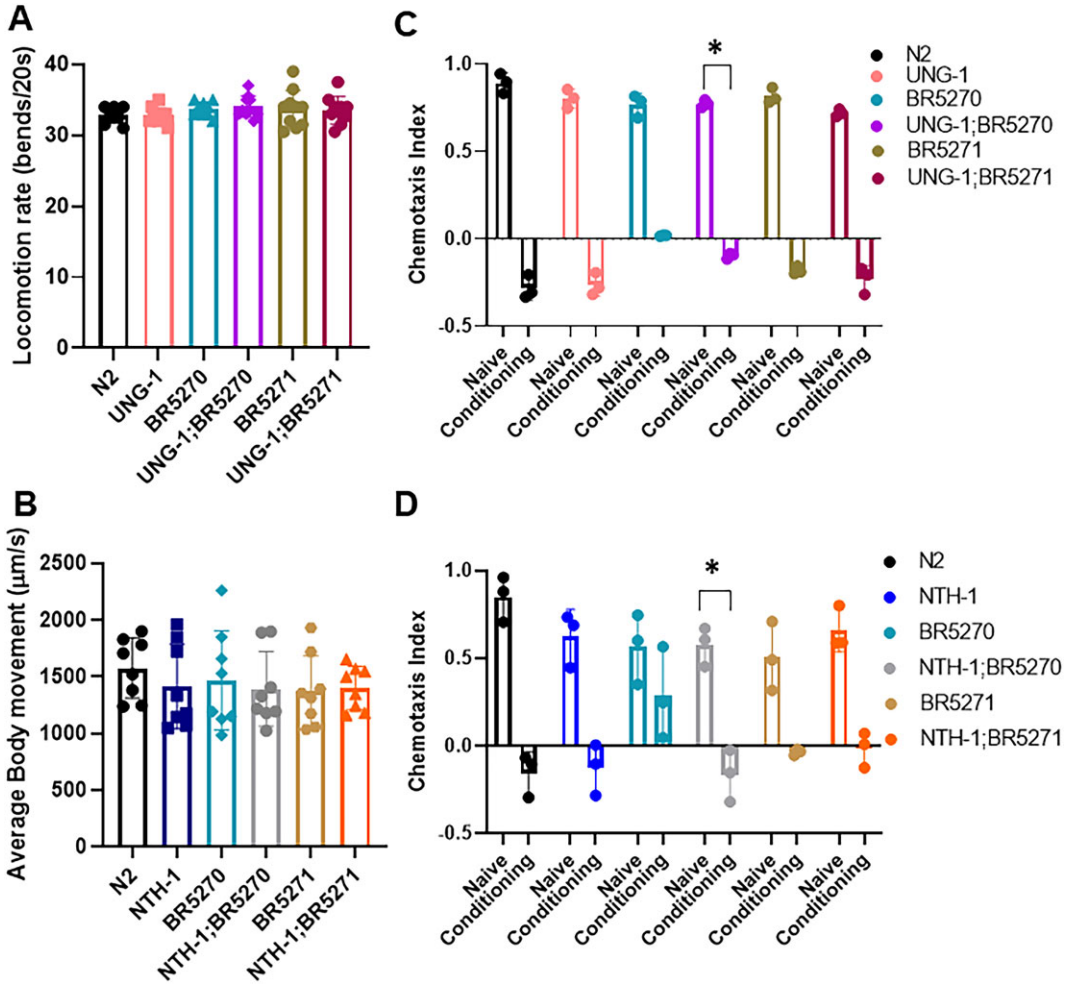

Figure 3. Loss of DNA glycosylases improves neuroplasticity in tau-aggregation expressing worm. (**A**) Locomotion rate measured as body bends per 20 seconds in a droplet of M9 buffer for 1-day old wild type (N2), UNG-1, BR5270, UNG-1;BR5270, BR5271 and UNG-1;BR5271 animals ($N = 3$ biological experiments (30 worms total). (**B**) Average body movement on OP50 seeded NGM medium for 1-day old N2, NTH-1, BR5270, NTH-1;BR5270, BR5271 and NTH-1;BR5271 animals. Locomotion was captured at 15 frames per second rate for 1min ($N = 3$ biological experiments). (**C**) Chemotaxis assay in naïve and Isoamyl alcohol (IAA) conditioned N2, UNG-1, BR5270, UNG-1;BR5270, BR5271 and UNG-1;BR5271 worms ($n = 150$–300 total worms in three biological experiments). (**D**) Chemotaxis assay in naïve and Isoamyl alcohol (IAA) conditioned N2, NTH-1, BR5270, NTH-1;BR5270, BR5271 and NTH-1;BR5271 worms ($n = 150$–300 total worms in three biological experiments). Locomotion analyses were done by one-way ANOVA followed by Tukey's multiple comparison test. Chemotaxis data was analysed by two-way ANOVA followed by Tukey's multiple comparison test. Data showing ± SEM, $*P \leq 0.05$.

BR5271 versus N2 DE gene lists (Supplementary Figure S2A), leading to the identification of 317 DE genes that were common among the BR5270s comparisons, but were not present in the BR5271 lists. Out of these, 291 were up- and 26 were downregulated (Supplementary Figure S2B). This consensus list of DE genes was subjected to enrichment analysis. It resulted in 34 significantly changed terms for the BR5270 versus N2 comparison and the top terms were largely related to muscle and actin (Figure 5C and Supplementary Table S4). Other significantly changed terms included: immune system process, calmodulin binding, and cellular oxidant detoxification. We attempted to do a similar analysis for BR5271, but there were only seven genes conserved between the two BR5271 strains and that is too few genes for enrichment analysis (Supplementary Figure S2A and Supplementary Table S5).

We then proceeded to evaluate each glycosylase KO;tau strain double mutant relative to N2 as well, since this is the way the behaviour analysis is done. To focus on BR5270 tau-pathology genes, we removed any DE genes that were also DE in the corresponding glycosylase KO;BR5271 comparisons (Supplementary Figure S2C and D). The resultant gene lists were then subjected to gene enrichment analysis (Supplementary Tables S6 and S7). UNG-1;BR5270 versus N2 (Supplementary Table S6) showed 15 terms, including defence response, lytic vacuole, immune system process, and response to axon injury. In comparison, NTH-1;BR5270 versus N2 (Supplementary Table S7) showed 78 terms, which included recombinational repair, DNA-directed DNA polymerase, metabolic processes, cell death, splicing, and multiple muscle and actin terms. Both glycosylase KO;BR5270 versus N2 comparison shared the terms response to axon injury and ABC-type transporter activity. Furthermore, a conserved set of genes was derived from the two glycosylase;BR5270 versus BR5270 comparisons (72 genes) and this consensus gene set was subjected to enrichment analysis (Figure 5D and Supplementary Table S8). Immune system process, defence response, and ABC-type transporters were the top changed terms.

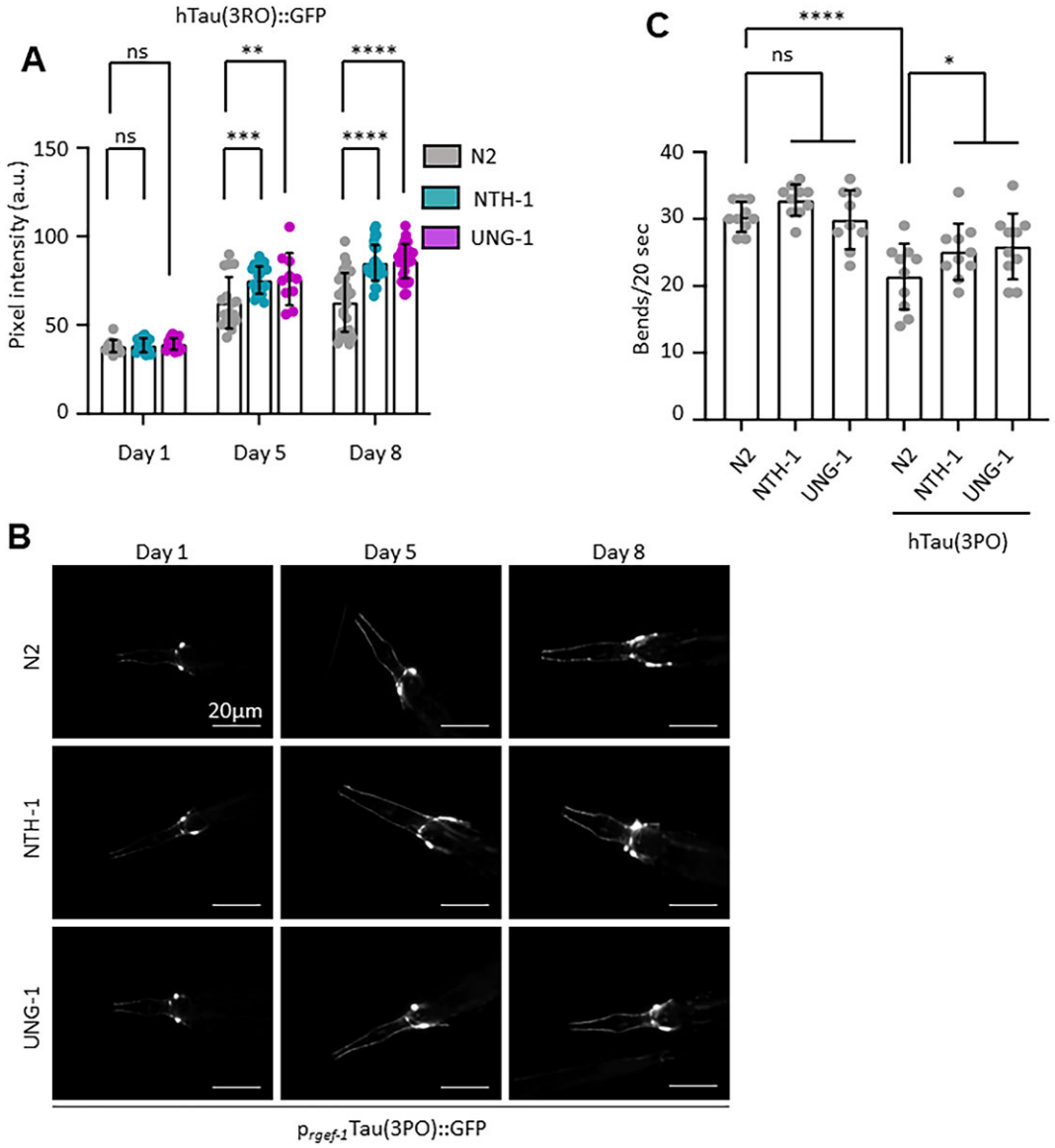

Figure 4. DNA glycosylases deficiency improves locomotion and enhances aggregation in tau-aggregation expressing nematodes. Transgenic nematodes expressing pan-neuronally the human Tau(3PO) isoform fused with GFP display progressive aggregates accumulation and locomotion impairment. (**A**) Both UNG-1 and NTH-1 deficiency increases the Tau(3PO)::GFP signal in 5-day and 8-day adults compared to their respective controls, indicating enhanced aggregation. (**B**) Representative images of the head region of Tau(3PO)::GFP expressing animals show age-related accumulation of aggregates that is enhanced in UNG-1 and NTH-1 animals. (**C**) Locomotion rate of nematodes expressing Tau(3PO). Body bends per 20 sec measured in M9 droplet ($n = 30$ nematodes per group). Data showing ± SEM. ns $P > 0.05$, $*P \leq 0.05$, $**P \leq 0.01$, $***P \leq 0.001$, $****P \leq 0.0001$. Statistical analysis was performed by one-way ANOVA followed by Tukey's multiple comparison test. Scale bars, 20 µm.

We also sought to focus on the gene changes altered in the UNG-1;BR5270 versus BR5270 and NTH-1;BR5270 versus BR5270 comparisons. UNG-1 and NTH1 invoked a similar number of DE genes in these comparisons, 570 and 544 genes, respectively (Supplementary Table S2). We evaluated these comparisons individually and then intersected the gene sets to find a conserved list of changed genes. Supplementary Tables S9 and S10 show the full list of enriched terms for UNG-1;BR5270 versus BR5270 and NTH-1;BR5270 versus BR5270, respectively. By this analysis, there were five conserved terms between the two lists of enrichment terms: myofibril, supramolecular polymer, actin-binding, organic acid transport, and structural constituent of the cytoskeleton. To further focus on aggregation-related pathology, we subsequently compared all glycosylase KO;BR5270 versus BR5270 DE gene lists and removed the set of glycosylase KO:BR5271 versus BR5271 DE genes, (Supplementary Figure S2E and F) ultimately producing a set of consistently deregulated genes, 6 up- and 141 downregulated. This list of DE genes was subjected to enrichment analysis and only two terms were identified as changed, homologous recombination (*P*-value 0.00041, *q*-value 0.12) and actin binding (*P*-value 0.00062, *q*-value 0.12).

Three genes were found in the term: *rfs-1* (*C30A5.3*), *cin-4* (*ZK1127.7*), and *rmh-2* (*T07C12.12*). All were upregulated in the BR5270 strains and after crossing with the glycosylase-deficient strains their expression was more normalized. To confirm the observed changes in the expression patterns of these three genes, we conducted qRT-PCR analysis in the respective genetic backgrounds. Our findings revealed an

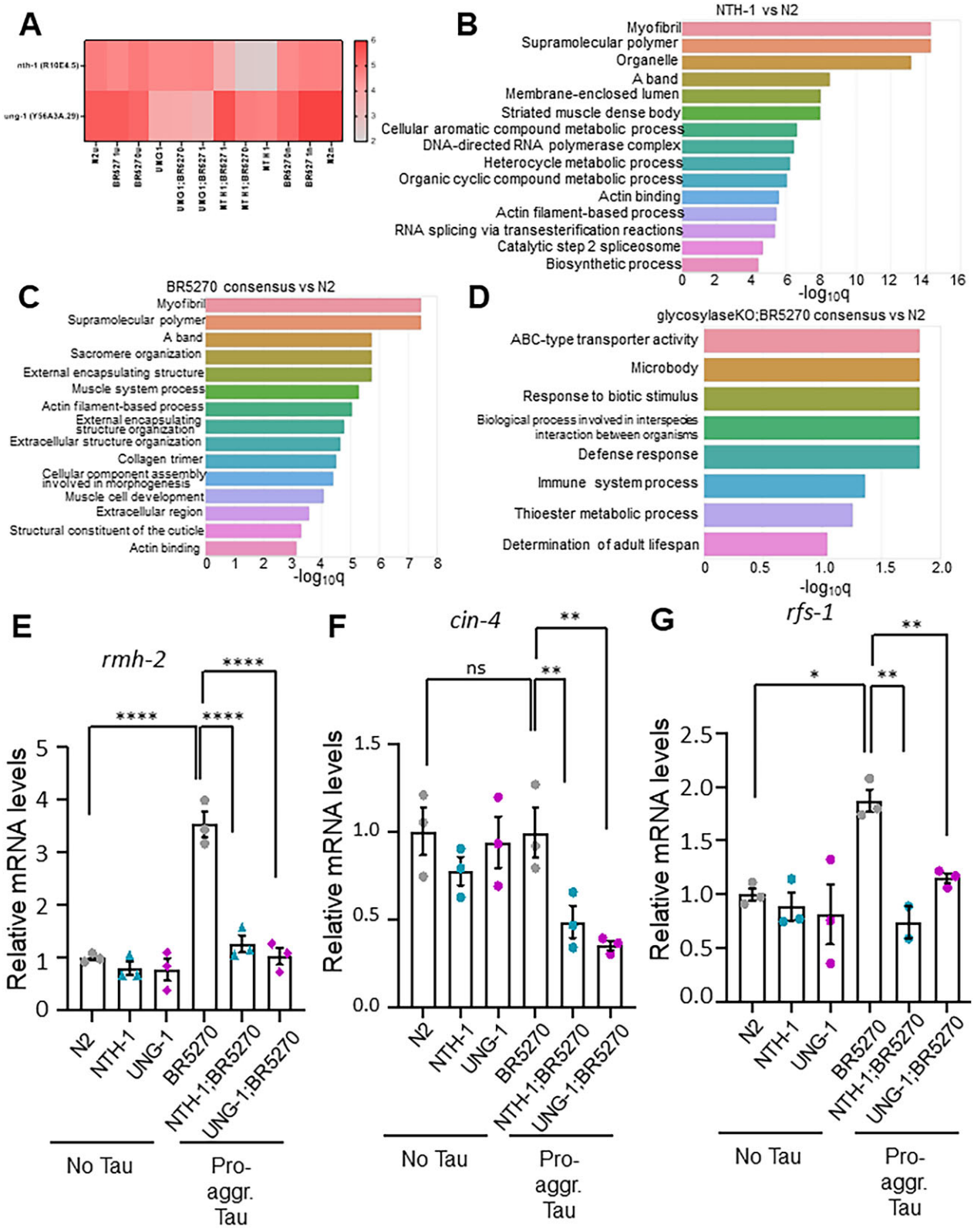

Figure 5. The transcriptomic analysis of DNA glycosylases deficient tau-aggregation expressing worms. (**A**) Glycosylase expression in the strains. Log^2 FPKM values for the respective strains, no normalization. (**B**) Gene enrichment analysis for NTH-1 versus N2. (**C**) Gene enrichment analysis for the shared set of genes found in both BR5270 versus N2 comparison. (**D**) Gene enrichment analysis for the shared set of genes found in both glycosylase KO;BR5270 versus BR5270 comparison. (**E–G**) mRNA levels of *rmh-2*, *cin-4* and *rfs-1* measured in the 'No Tau' expressing strains N2, NTH-1, UNG-1 and the 'Pro-aggregation Tau' expressing strains BR5270, NTH-1;BR5270, UNG-1;BR5270. Data showing ± SEM. ns $P > 0.05$, $*P \leq 0.05$, $**P \leq 0.01$, $***P \leq 0.001$, $****P \leq 0.0001$. Statistical analysis was performed by one-way ANOVA followed by Tukey's multiple comparison test.

upregulation in the expression of *rmh-2 (T07C12.12)*, and *rfs-1 (C30A5.3)* in the BR5270 strain, while *cin-4 (ZK1127.7)* is not affected (Figure 5E–G). Furthermore, upon the genetic ablation of NTH-1 and UNG-1, the expression levels of these genes reverted to those observed in the wild type strain (Figure 5E and G).

Additionally, we compared our worm tauopathy vs N2 DE genes lists (317, of which 307 could be mapped to human/mouse genes) with a human AD dataset (26) and a mouse AD dataset (27). The human data set was derived from the entorhinal cortex whereas the mouse model was from neocortex of the Tg2576 AD model which overexpresses a mutant form of APP leading to amyloid pathology. BR5270 worms had similar terms to those found in humans such as: actin filament-based process, calcium signalling, and regulation of immune response. Upon combining the human DE gene list from the various cell types and comparing to our consensus BR5270 versus N2 gene list, we found 5 overlapping entries. These were CNTN2, DLC2, PLCE1, SLC8A1, and COL21A1. These genes either do not appear or are negative for an association with Alzheimer's disease in the Alzgene database (alzgene.org). Additionally, we compared our DE gene list to a multicell analysis of the Tg2576 mouse model. Here we identified 7 genes overlapping: CNTN2, SOX2, ENPP2, HPGDS, MYO6, TUBB4A, and KL. CNTN2 (contactin 2) was shared between all three data sets and encodes a glycoprotein important in axonal guidance, proliferation, and migration in neurons. Notably, in a small previous study, expression of contactin 2 showed differences between mild cognitively impaired AD individuals and controls (38). In the *C. elegans* dataset, this gene was upregulated in the BR5270_N2 comparisons (over 3-fold *P*-values 2.91E-11 and 5.06E-14 for UNG-1-set and NTH-1-set, respectively) and was not a DE gene in the BR5271 versus N2 comparisons. The gene's expression went down in UNG1;BR5270 but remained high in the NTH1;BR5270 versus N2 comparisons. The fact that this gene is found across species might make it a candidate for further analysis.

NTH-1 deficiency promotes resistance to DNA damaging agents

To elaborate further the role of DNA glycosylases in organismal physiology and survival under conditions of oxidative DNA damage, adult nematodes were subjected to 1mM menadione, a potent inducer of oxidative stress. Animals were maintained on menadione-treated plates throughout their lifespan to examine the specific contribution of DNA glycosylases in mitigating the adverse consequences of oxidative DNA lesions and assess their significance in promoting overall organismal health and survival (Figure 6 and Supplementary Table S1). The lifespan of tau-expressing nematodes (BR5270) was reduced significantly as compared to other strains. Although the lifespan of UNG-1 was unaffected upon menadione treatment, UNG-1 depletion reduced the viability of both tau-expressing strains (median lifespan 8 days) highlighting the pivotal role of UNG-1 in the response to oxidative damage (Figure 6A, C, E and G, Supplementary Table S1). Interestingly, in contrast to UNG-1 deficient worms, all NTH-1 deficient genotypes exhibited increased lifespan as compared to their respective counterparts (median lifespan of BR5270 – 8 days and NTH-1;BR5270 – 15 days) (Figure 6B, D, F and H, Supplementary Table S1). Notably, the different survival rates between UNG-1 and NTH-1 deficient worms upon menadione exposure may be explained by the subcellular location and the function of these two DNA glycosylases. UNG-1 is a monofunctional DNA glycosylase that is present in the nucleus, whereas NTH-1 is a bifunctional DNA glycosylase that is located both in the nucleus and mitochondria (12). In the absence of UNG-1, NTH-1 may take over the role of UNG-1 to repair oxidative DNA damages. Thus, we investigated whether there is any compensatory function between UNG-1 and NTH-1 DNA glycosylases (Supplementary Figure S3). Notably, the depletion of NTH-1 does not influence the mRNA levels of *ung-1* (Supplementary Figure S3E). Similarly, the ablation of UNG-1 does not affect the levels of *nth-1* mRNA (Supplementary Figure S3F). Moreover, silencing of *nth-1* by RNAi did not affect neither the levels nor the localization of a chimeric UNG-1::mCherry protein, which remained exclusively nuclear (Supplementary Figure S3C and D). These findings are consistent with our RNA-seq data, indicating the absence of a compensatory mechanism following the loss of either DNA glycosylase. This lack of compensation further enhanced the notion that NTH-1 and UNG-1 operate independently within the cellular environment, without any detectable cross-regulation and/or functional redundancy. To this direction, our RNAseq analysis demonstrates that NTH-1 has a major role in transcription regulation (Figure 5).

It is reported that the loss of NTH-1 activity helps in restoring the short lifespan of *C. elegans* mutants defective for XPA-1/Xeroderma pigmentosum group A, which plays a pivotal role in the nucleotide excision repair (NER) pathway. Furthermore, loss of function of NTH-1 (BER) and XPA-1 (NER) proteins lead to an oxidative stress response and global change in gene expression (39). This suggests that certain DNA damages are recognized by NTH-1 but are processed by XPA-1 through the NER pathway. Previously, we have shown that Cockayne syndrome group B (CSB) protein stimulates repair of BER substrate by NEIL1 DNA glycosylase (40). Given the limited number of DNA repair proteins in *C. elegans* and the cross-talk between them, we investigated the interplay between the BER and nucleotide excision repair (NER) pathways (41). To monitor their overlapping functions, we generated specific DNA lesions, such as UVC-induced cyclobutane pyrimidine dimers (CPDs) and cisplatin-induced crosslinks (42). By studying the repair outcomes and efficiency in response to these distinct substrates, we tried to uncover the pivotal function of BER and NER pathways in the maintenance of nematode genomic integrity. We subjected worms to a total dose of 75J/m^2 and followed their lifespan (Figure 7). Both tau-expressing strains exhibited a short lifespan after irradiation in comparison to N2 animals (Figure 7A and B, Supplementary Table S1). We detected no significant differences between wild type N2 and UNG-1 deficient worms (Figure 7A and C), but there was a trend towards increased survival of UNG-1 deficient tau-expressing worms (UNG-1;BR5271 and UNG-1;BR5270) (median lifespan 10 days) as compared to their respective controls (BR5271 and BR5270) (median lifespan 9 days) (Figure 7A, E and G, Supplementary Table S1). Similarly, there were no significant differences between wild type N2 and NTH-1 deficient animals (Figure 7B and D). In contrast, there was a significant increase in the survival of both NTH-1 deficient tau-expressing nematode strains (NTH-1;BR5271 and NTH-1;BR5270), which was more pronounced in the strain expressing the aggregation-prone from of the protein (NTH-1;BR5270), (median lifespan

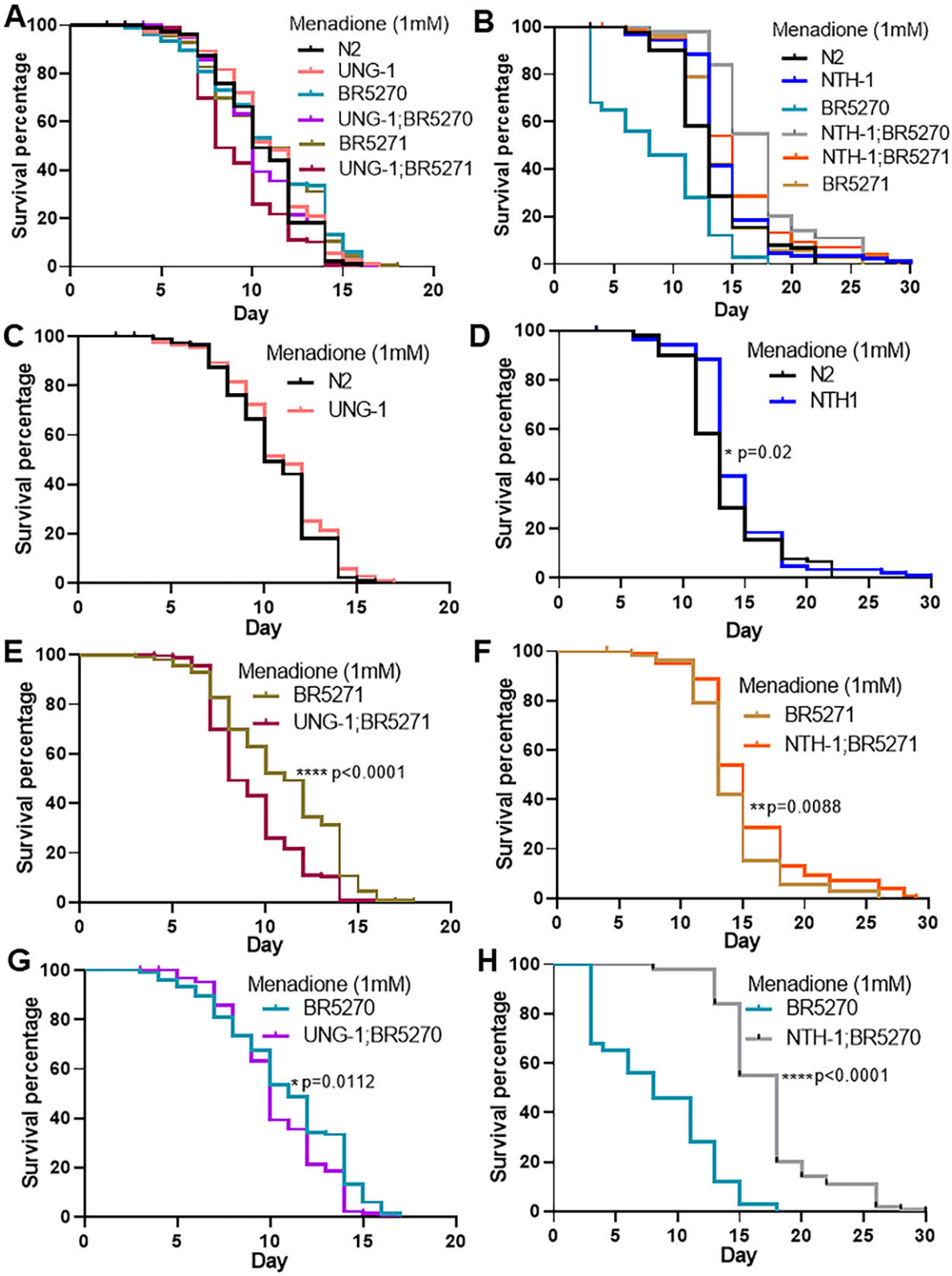

Figure 6. NTH-1 glycosylase mutant shows an extended healthy lifespan in tau-aggregation expressing worms under menadione induced oxidative stress. Lifespan of (**A**) wild type (N2), UNG-1, BR5270, UNG-1;BR5270, BR5271 and UNG-1;BR5271, (**B**) N2, NTH-1, BR5270, NTH-1;BR5270, BR5271 and NTH-1;BR5271, (**C**) N2 and UNG-1, (**D**) N2 and NTH-1, (**E**) BR5271 and UNG-1;BR5271, (**F**) BR5271 and NTH-1;BR5271, (**G**) BR5270 and UNG-1;BR5270, (**H**) BR5270 and NTH-1;BR5270 at indicated menadione concentration. Statistical analyses were performed on Kaplan–Meier survival curves by Logrank (Mantel–Cox) tests (See Supplementary Table S1 for detailed *P*-value). $*P \leq 0.05$, $**P \leq 0.01$, $****P \leq 0.0001$ ($n = 20$ worms/study; total of 100 worms).

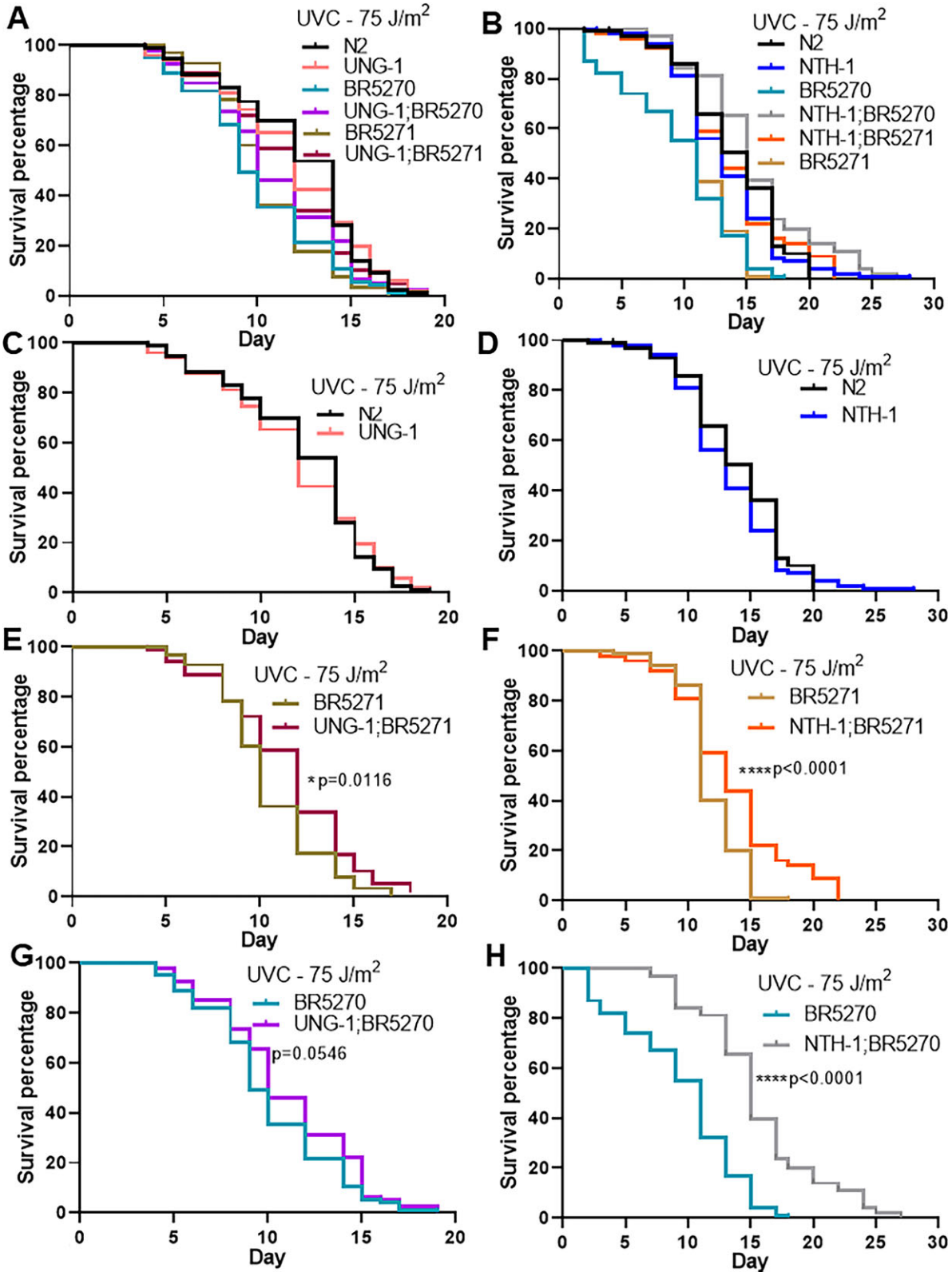

Figure 7. NTH-1 glycosylase mutant shows an extended healthy lifespan in tau-aggregation expressing worm after UVC insult. Lifespan of (**A**) wild type (N2), UNG-1, BR5270, UNG-1;BR5270, BR5271 and UNG-1;BR5271, (**B**) N2, NTH-1, BR5270, NTH-1;BR5270, BR5271 and NTH-1;BR5271, (**C**) N2 and UNG-1, (**D**) N2 and NTH-1, (**E**) BR5271 and UNG-1;BR5271, (**F**) BR5271 and NTH-1;BR5271, (**G**) BR5270 and UNG-1;BR5270, (**H**) BR5270 and NTH-1;BR5270 at indicated UVC dose. Statistical analyses were performed on Kaplan–Meier survival curves by Logrank (Mantel–Cox) tests (See Supplementary Table S1 for detailed *P*-value) $*P \leq 0.05$, $****P \leq 0.0001$ ($n = 20$ worms/study; total of 100 worms).

15 days) as compared to their respective controls (BR5271 and BR5270) (median lifespan 11 days) (Figure 7B, F and H, Supplementary Table S1).

In addition to the aforementioned UVC-induced CPDs, we expanded our analysis and treated NTH-1 deficient nematodes with cisplatin, another DNA damaging agent that causes DNA crosslink lesions, known to be repaired by the NER pathway (Figure 8). Here, we did not observe any difference between the survival of wild type (N2) animals and neither tau-expressing strains nor NTH-1 deficient worms (Figure 8A and B). Notably, NTH-1 deficient tau-expressing animals (NTH-1;BR5270) (median lifespan 18 days) were more resistant to cisplatin supplementation compared to their respective controls (BR5270) (median lifespan 14 days; Figure 8D and Supplementary Table S1). These results indicate that the NTH-1 DNA glycosylase modulates NER and/or promotes recombinational repair to facilitate recovery from NER-repaired lesions.

ROS signaling is partially responsible for the altered gene expression profile of NTH-1 deficient mutants

It was established that nematodes lacking NTH-1 display heightened basal levels of ROS, which play an essential role in the regulation of several stress response genes by orchestrating the transcription efficiency and mitochondrial metabolism (18,19). Thus, we sought to determine whether the protective effect against oxidative stress could be reversed upon ROS scavenger administration. To examine this hypothesis, we assessed the brood size and viability of the NTH-1 deficient worms in the presence and absence of *N*-acetyl-L-cysteine (NAC), a well-known ROS scavenger (Figure 9). The presence of NAC did not affect the pattern of brood size (Figure 9A and B) or egg viability (Figure 9C and D) in these worms as observed under otherwise normal conditions. We further measured the effect of NAC after menadione-induced oxidative damage (Figure 9E–I). We found that NAC supplementation suppressed the increased lifespan of NTH-1 deficient worms under menadione treatment (median lifespan from 18 days to 13 days; compare Figure 9E and F with Figure 6B and D, Supplementary Table S1). Moreover, NAC supplementation reduced the positive effect of NTH-1 deletion on the lifespan of menadione treated tau-expressing nematodes (median lifespan 15 days; Figure 9H, Supplementary Table S1), as compared to an extension of lifespan of menadione alone treated tau-expressing nematodes (median lifespan 18 days; (Figure 9I, Supplementary Table S1). These findings suggest that the altered transcriptional profile, memory improvement and increased survival rate of the tau-expressing nematodes upon NTH-1 deficiency is partially regulated via the level of free radical generation (Figures 5 and 9).

NTH-1 deficiency reduces DNA damage accumulation and improves mitochondrial homeostasis

To investigate whether the observed improvement in memory was associated with a reduction in the accrual of DNA damage, we monitored the endogenous levels of 8-hydroxyguanine (8-oxoG), a marker of oxidized DNA bases, in wild-type and NTH-1 deficient tau-expressing nematodes by utilizing immunohistochemical staining with anti-8-oxoG antibodies (12). Interestingly, we observed that wild type (N2) worms and NTH-1 deficient worms displayed similar levels of 8-oxoG, indicating comparable levels of DNA damage. In contrast, tau-expressing nematodes demonstrated increased signal indicating enhanced levels of oxidized DNA bases (Figure 10A and B). Notably, NTH-1 deficiency significantly reduced the increased level of 8-oxoG that were detected in the tauopathy nematode model. These results suggest that NTH-1 deficiency can mitigate the accumulation of oxidized DNA bases in tau-expressing worms, potentially providing a mechanistic link between NTH-1 activity, DNA damage, and improved longevity in this model.

To assess the accumulation of single-stranded DNA (ssDNA) breaks, we utilized the TUNEL assay, which measures the incorporation of labelled dUTP at 3-OH single-stranded DNA ends, crucial intermediates in the BER pathway. Both wild type (N2) and NTH-1 deficient nematodes displayed low levels of endogenous TUNEL signal (Figure 10C and D). However, in the tau-expressing worms (BR5270), a high level of endogenous TUNEL signal was identified, which was significantly reduced in NTH-1 deficient tau-expressing worms (NTH-1;BR5270) (Figure 10C and D). Taken together, these data suggest that endogenous DNA damage is higher in the tau-aggregation expressing strain. By comparing the results between BR5270 and NTH-1;BR5270, we suggest that NTH-1 modulates the induction and/or repair of some endogenous DNA damage, potentially leading to the accumulation of ssDNA breaks. Consequently, NTH-1 DNA glycosylase loss diminishes the accumulation of mutagenic 8-oxoG lesions and single-strand breaks, which are precursors to toxic double-strand breaks, thereby conferring a benefit for the organism.

The interplay between DNA damage and mitochondrial defects has been recognized as a crucial factor in neurodegenerative pathologies, including Alzheimer's disease (AD) (31,43). To assess mitochondrial function, we utilized TMRE (tetramethylrhodamine ethyl ester) as an indicator to evaluate mitochondrial membrane potential (44) (Figure 11 and Supplementary Figure S4). Interestingly, there was no significant differences in mitochondrial membrane potential between wild type (N2), UNG-1 and NTH-1 deficient animals as they aged (Figure 11). In contrast, tau-expressing nematodes exhibited a significant difference in mitochondrial activity from day 1 to day 7 compared to wild type (N2) worms. For instance, there was a significant difference in TMRE staining between wild type (N2) and BR5270 worms of each UNG-1 and NTH-1 set at day 1 (34.03% in the NTH-1 set - Figure 11A and B, 35.55% in the UNG-1 set - Figure 11C and D). Notably, NTH-1 deficiency rescued this loss of membrane potential in tau-expressing worms (NTH-1;BR5270) (Figure 11A and B). This effect was also observed at day 1 for UNG-1;BR5270 worms, but did not remain significant in the aged nematodes (Figure 11C). Taken together, these results highlight the pivotal role of NTH-1 in the maintenance of mitochondrial function. The same is also true for UNG-1 in early life stages but not in aged individuals. Further investigations are warranted to explore the impact of DNA glycosylases, especially NTH-1, on mitochondrial metabolism in tauopathies.

Discussion

Alzheimer's Disease (AD) is one of the most common neurodegenerative diseases and it involves clinical features of cognitive defects later in life, disorientation, and behavioural issues. Aging is a major risk factor for the development and

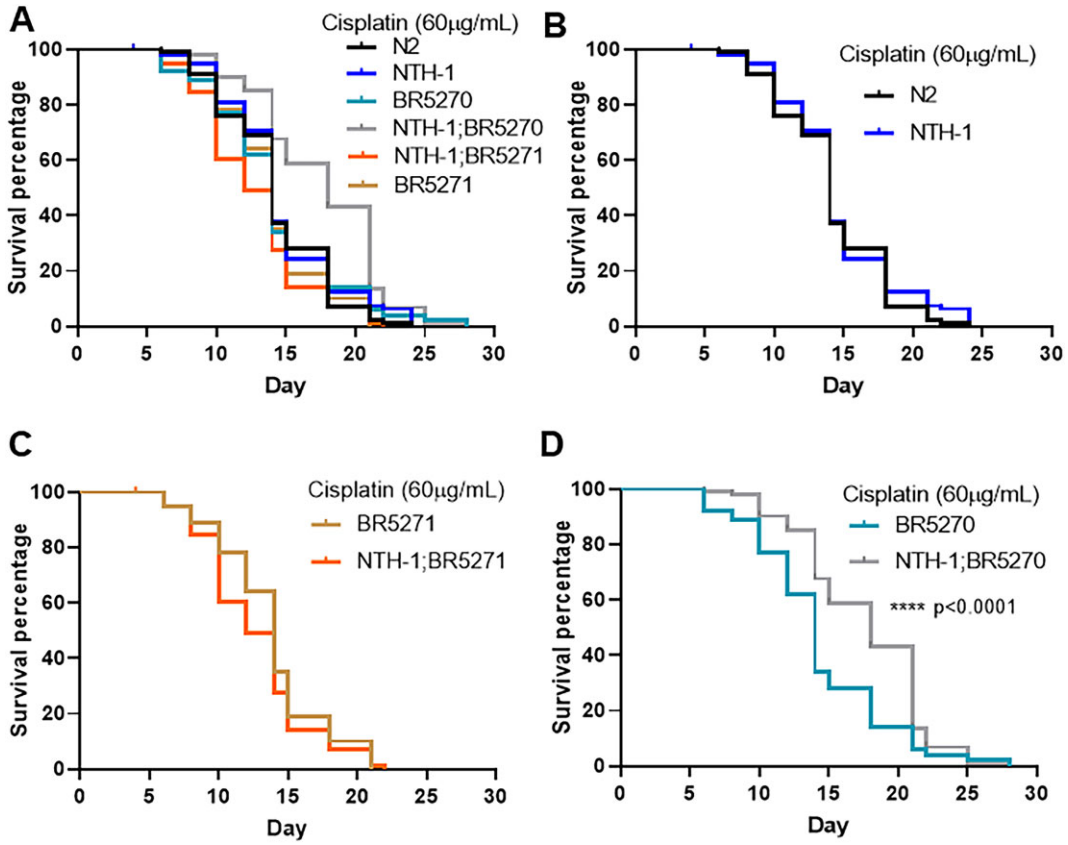

Figure 8. NTH-1 deficiency shows an extended healthy lifespan in tau-aggregation expressing worm upon cisplatin induced DNA damage. Lifespan of (**A**) wild type (N2), NTH-1, BR5270, NTH-1;BR5270, BR5271 and UNG-1;BR5271, (**B**) N2 and NTH-1, (**C**) BR5271 and NTH-1;BR5271, (**D**) BR5270 and NTH-1;BR5270 at indicated cisplatin dose. Lifespan statistical analyses were performed on Kaplan-Meier survival curves by Logrank (Mantel-Cox) tests (See Supplementary Table S1 for detailed *P*-value), $****P < 0.0001$ ($n = 20$ worms/study; total of 100 worms).

progression of AD (45). Using the nematode *C. elegans*, we demonstrated that DNA glycosylase-mediated initiation of the base excision repair (BER) pathway promotes the accumulation of DNA repair intermediates, such as abasic sites, nicks, and unrepaired single-stranded DNA breaks, which are closely associated with neurodegeneration (Figure 12). Notably, in NTH-1 deficient tau-expressing nematodes, the accumulation of DNA repair intermediates is attenuated. We suggest that reduced activity of BER DNA glycosylases can be beneficial and/or neuroprotective during aging. While this is the first such demonstration in a tauopathy model, previous studies have also supported this notion. AAG-deficient mice showed protection against alkylating agents (11). Other than its DNA repair enzymatic activity, AAG is also involved in alkylation-induced unfolded protein response (UPR) activation (46). Similarly, a recent study showed that a catalytically inactive mutant of 8-oxoguanine DNA glycosylase (OGG-1) acts as a potent regulator of gene expression. This OGG-1 driven transcription regulation is dependent on its substrate binding ability (47).

Various animal model systems have been used to study AD, including *C. elegans* (48). AD worms have several features of the human pathology, including memory loss, increased oxidative stress, neuronal loss and deficient mitophagy (49–51). Studies in various model systems suggest that both increased DNA damage and reduced DNA repair can aggravate AD phenotypes (52–55). Further studies demonstrated lower levels of expression of uracil DNA glycosylase, β-OGG-1 glycosylase, and Polβ in AD brains as compared to-age matched controls (7,10,56,57). Polβ deficiency is associated with neurodegeneration in mice (10). Our past work-based studies in mice and cells suggests that BER DNA repair intermediates themselves serve as catalysts, which drive aging and age-associated diseases including neurodegeneration (56,58).

The RNAseq data presented here demonstrate that other than its DNA repair activity, NTH-1 may be involved in the regulation of the spliceosome. Spliceosomes are large ribonucleoprotein (RNP) complexes which excise introns from pre-messenger RNA (pre-mRNA) to synthesize mRNA for translation. 99.5% of introns are removed by the major spliceosome, which consists of U1, U2, U4, U6 and U5 small nuclear RNAs (snRNAs), whereas the remaining 0.5% introns are taken care of by the minor spliceosome. Mature spliced mRNAs are created through assembly of the splicing machinery, in which U1 snRNP recognizes the beginning of an intron (5′ splice site) and U2 snRNP is involved in identification of the branch site at the other end (59). Through a cascade of reactions involving various other factors, the spliceosome disassembles from the excised intron, which is then debranched and degraded (59). Spliceosome proteins aggregate and localize to tau neurofibrillary tangles, which makes splicing disruption a hallmark of AD (60,61). Alternative splicing of pre-mRNA contributes significantly to the functional diversity and complexity of proteins expressed in tissues, especially in brain (60). Previous proteomic analysis of AD brain samples showed significant accumulation of insoluble U1 snRNP (62). This GO

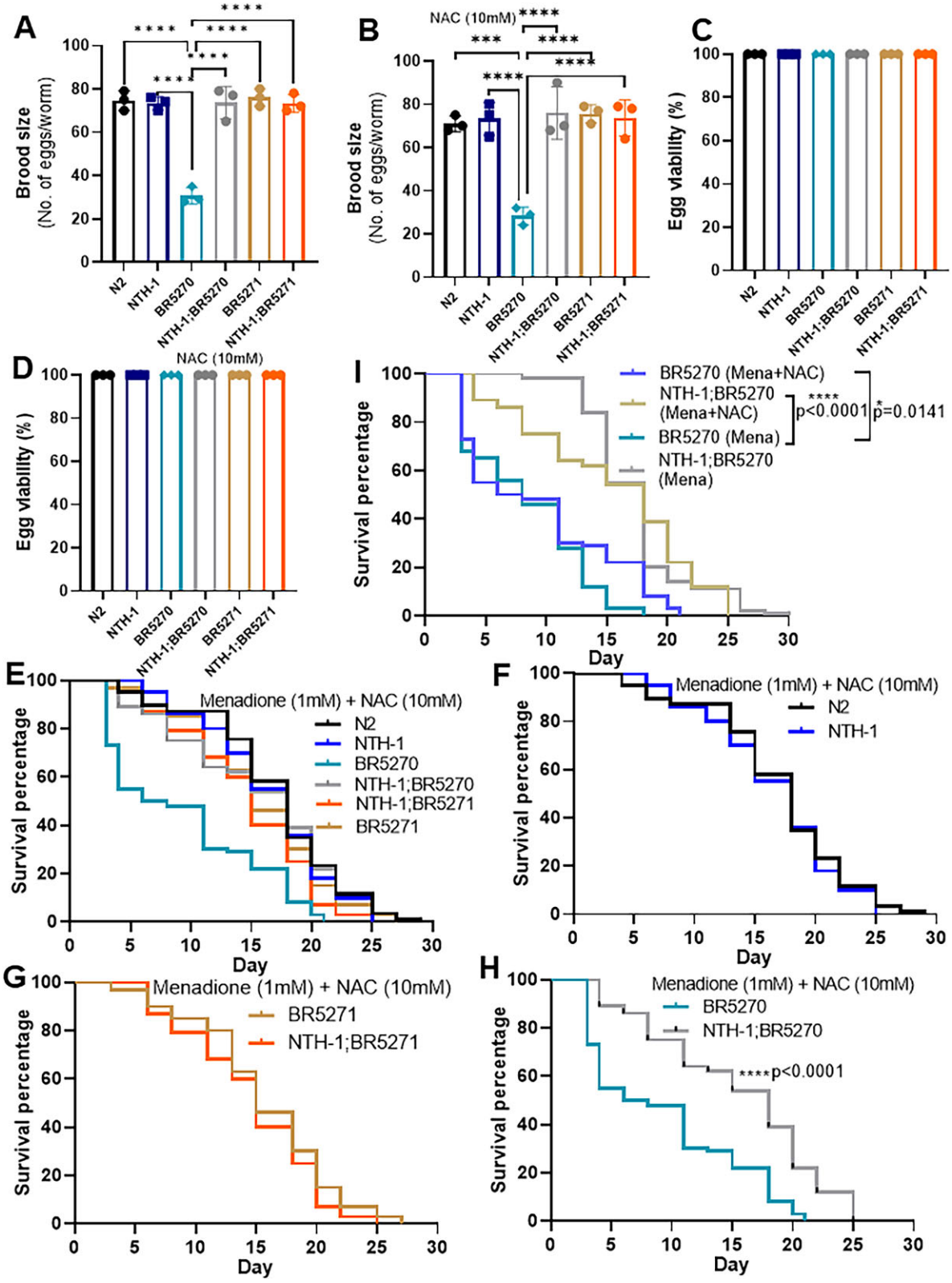

Figure 9. Basal level ROS is partially responsible for the improved stress response of tau-expressing animals with NTH-1 depletion. **(A, B)** Brood size of day 1 adult N2, NTH-1, BR5270, NTH-1;BR5270, BR5271 and NTH-1;BR5271 worms in the absence and the presence of the indicated NAC concentration ($n = 3$–5 worms for each replicate). **(C, D)** Egg viability measured 24h after brood size in N2, NTH-1, BR5270, NTH-1;BR5270, BR5271 and NTH-1;BR5271 worms in the absence and the presence of the indicated NAC concentration. (**E–H**) Lifespan analyses of N2, NTH-1, BR5270, NTH-1;BR5270, BR5271 and NTH-1;BR5271 (**I**) Lifespan analyses of menadione treated BR5270 and NTH-1;BR5270 in presence and absence of NAC. Brood size and viability statistical analyses were by one-way ANOVA followed by Tukey's multiple comparison test. Data showing ± SEM. Three biological experiments were performed. Lifespan statistical analyses were performed on Kaplan–Meier survival curves by Logrank (Mantel-Cox) tests (see Supplementary Table S1 for detailed *P*-value) ($n = 20$ worms/study; total of 100 worms). $*P \leq 0.05$, $***P \leq 0.001$ and $****P < 0.0001$.

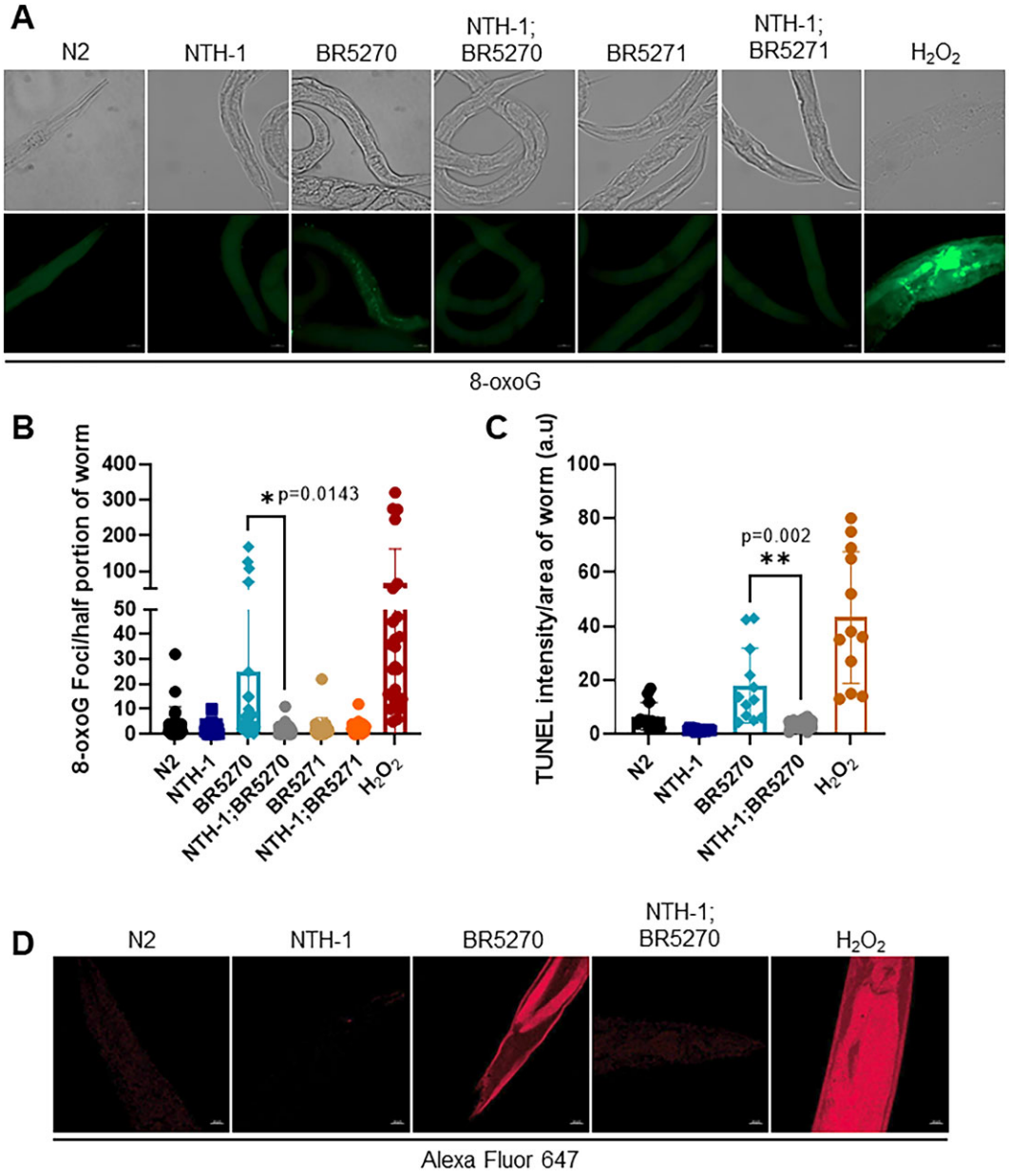

Figure 10. NTH-1 deficiency diminishes genomic damage in tau-aggregation expressing worm. (**A, B**) Representative images and graph showing the number of 8-oxoG positive foci in the half portion of N2, NTH-1, BR5270, NTH-1;BR5270, BR5271 and NTH-1;BR5271 worms. (**C, D**) Graph and images showing the intensity of TUNEL positive staining/area of N2, NTH-1, BR5270, NTH-1;BR5270, BR5271 and NTH-1;BR5271 worms. $n = 25$ worms per condition. Statistical analysis was performed by unpaired *t*-test. $*P \leq 0.05$.

term was significantly changed in the nematodes along with regulation of synaptic structure or activity. Thus, widespread splicing disruption affects brain transcriptomes including Aβ and tau protein. Hence interference in RNA metabolism including mRNA splicing, is associated with age-related disorders like AD (63,64). HSP-70 is another spliceosome protein, a part of Prp19 splicing complex, found upregulated in NTH-1;BR5270 (65). *C. elegans* HSP-70 protein is constitutively expressed throughout life and its expression increases under stress conditions (66,67). This chaperone protein regulates longevity and maintains the cytoplasmic folding environment in *C. elegans* (68). Knockdown of heat shock protein promotes accumulation of polyglutamine aggregates in transgenic *C. elegans* strains (69). We believe that upregulation of the spliceosome in NTH-1 mutant worms, which involves the HSP-70 family of proteins, may be involved in proper assembly of the spliceosome complex or prevent isolation of key components in the tau neurofibrillary tangles. It may also be involved in reducing the aggregation of proteins like tau. It will be interesting to study the effect of the spliceosome in DNA glycosylase mutant background on progression of AD phenotype in the future. In comparison to UNG-1 mutant worms, NTH-1 mutants had altered expression of many more genes. Further, the number of gene sets differentially regulated in NTH-1;BR5270 worms are greater than in BR5270 alone. We noted methylation and epigenetic regulation among the terms for NTH-1 and thus it may modulate gene expression via this mechanism, which is beyond the scope of this paper. Clearly, NTH-1 has additional functions in transcription regulation beyond its roles in DNA repair.

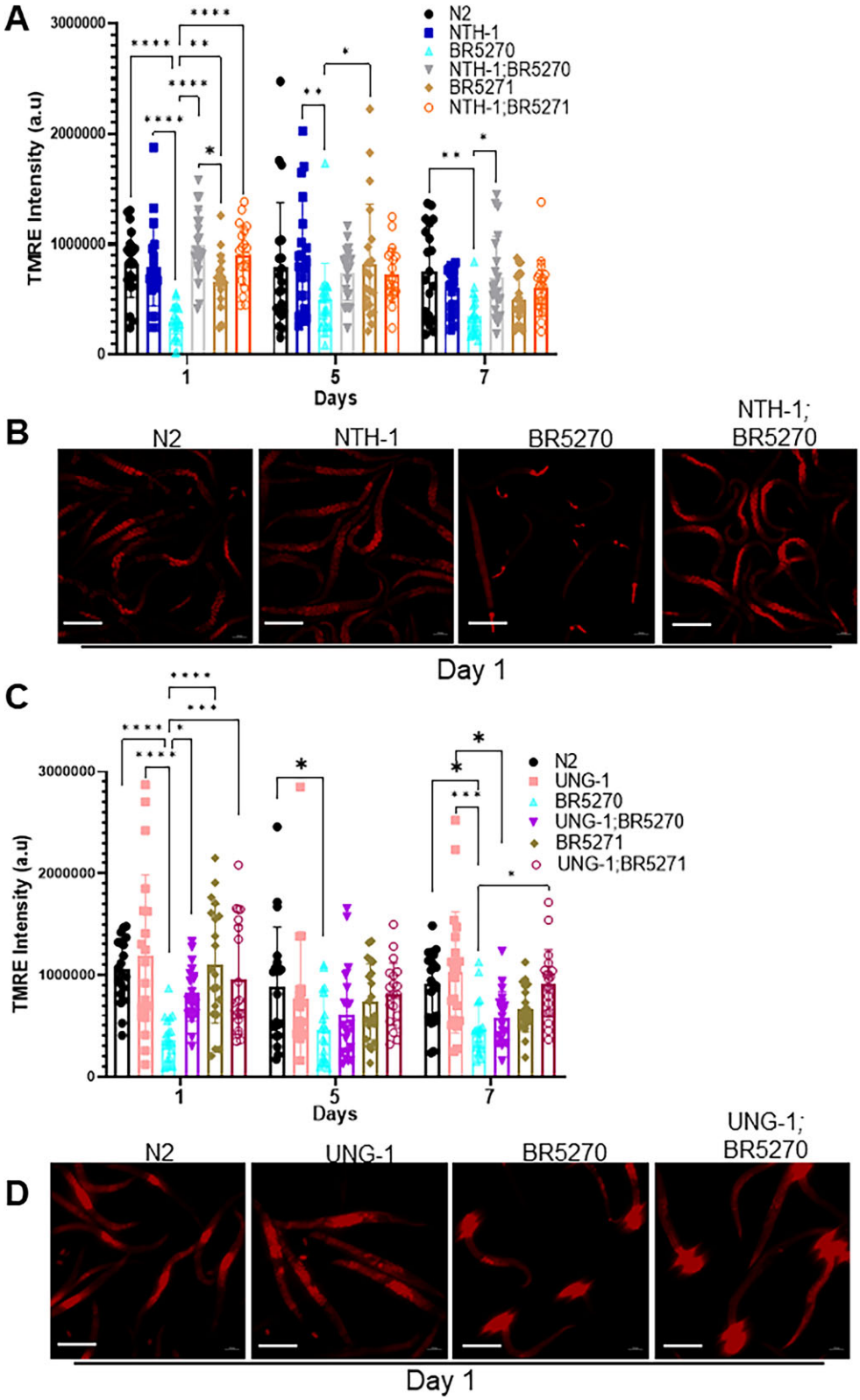

Figure 11. NTH-1 and UNG-1 deficiency improves mitochondrial membrane potential in tau-aggregation expressing nematodes. Fluorescence intensity and representative images of (**A, B**) N2, NTH-1, BR5270, NTH-1;BR5270, BR5271 and NTH-1;BR5271 animals and (**C, D**) N2, UNG-1, BR5270, UNG-1;BR5270, BR5271 and UNG-1;BR5271, incubated overnight with 200nM TMRE ($n = 20$ worms from two biological experiments). Data showing ± SEM, Statistical analysis was performed by two-way ANOVA followed by Tukey's multiple comparison test. $*P \leq 0.05$, $**P \leq 0.01$, $***P \leq 0.001$ and $****P \leq 0.0001$. TMRE fluorescence intensity was analysed using ImageJ. Additional representative images are shown in Supplementary Figure S4.

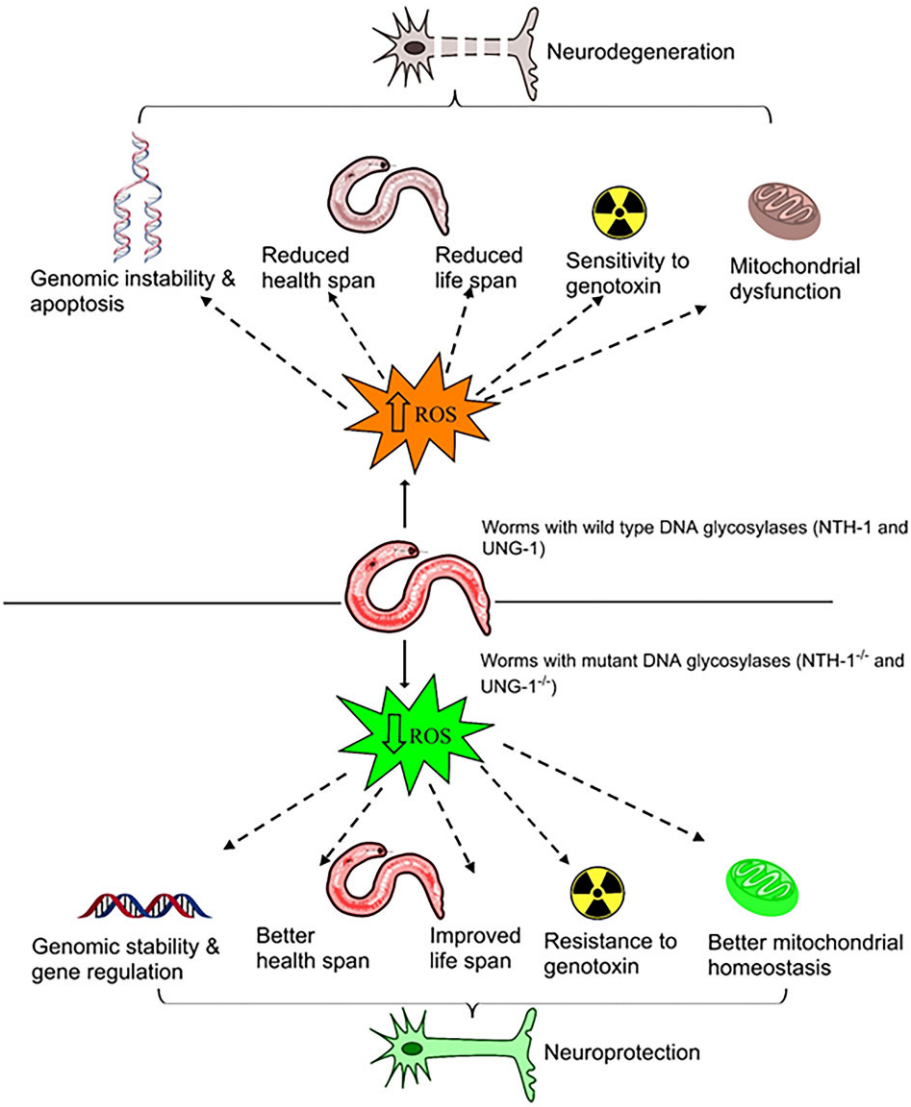

Figure 12. BER serves as a susceptibility modulator in *C. elegans* tauopathy model. Gradual accumulation of DNA damages via ROS or DNA glycosylase-mediated generation of DNA repair intermediates and incomplete DNA repair by BER, leads to persistent genomic stress, reduced health and lifespan, increased sensitivity to genotoxins and apoptosis, and mitochondrial dysfunction. The accumulation of DNA repair intermediates, such as abasic sites, nicks, and unrepaired single-stranded DNA breaks cause neuronal vulnerability and degeneration in tau-aggregation expressing animals. In DNA glycosylases mutant nematodes (UNG-1 and NTH-1-deficient), there is reduced generation of ROS and DNA repair intermediates due to reduced BER capacity that causes a reduction in apoptosis, improved health, and lifespan with better ability to deal with genotoxins and better mitochondrial homeostasis which helps in the maintenance and longevity of neurons, resulting in neuroprotection.

Several studies showed greater mobility impairment and severe neuronal dysfunction in a *C. elegans* expressing the aggregating tau species (30). Tau protein belongs to the family of microtubule-associated proteins (MAPs), which are involved in microtubule assembly. Tau supports microtubule stability, however, hyperphosphorylation detaches it from microtubules and leads to the formation of neurofibrillary tangles (15). Also, worms defective in DNA repair factors exhibit defective long- and short-term memory (20). We did not observe cognitive defects in DNA glycosylase deficient worms, but lack of these glycosylases improved cognitive behaviour in AD worms.

Data presented here show improved survival of old tau-aggregation expressing nematodes in the presence and absence of exposure to DNA-damaging agents. ssDNA breaks can be generated by several cellular mechanisms and resolved efficiently in early stages of life. However, an imbalance in the clearance of these intermediates contributes to damage in neurons and hence neurodegeneration occurs at later stages of development. Thus, exposure to these stressors is a reflection of the aging process. In NTH-1-deficient tau worms (NTH-1;BR5270), which likely have reduced initiation of BER in response to oxidative DNA damage, we observed increased lifespan, improved memory, and reduced accumulation of ss-DNA breaks. Similar results were observed in a nematode model of Parkinson's disease (12). In that study, *nth*-1;BY273 worms showed ssDNA break accumulation with age and reduced PARylation of proteins. They also observed stimulated mitohormesis through an LMD-3/JNK-1/SKN-1-dependent signalling cascade (12). Although we did not observe up-regulation of these genes in our RNAseq data, we observed increased mitochondrial membrane potential in NTH-1

deficient tau-aggregation expressing worms. This supports the idea that NTH-1 is involved in mitochondrial homeostasis. Consistent with this notion, our findings indicate that while the loss of DNA glycosylases ameliorates tau-induced phenotypes, it simultaneously promotes tau aggregation. This observation could be attributed to the activation of independent compensatory mechanisms involving mitochondria or to alterations that enhance mitochondrial tolerance to tau toxicity, scenarios that require further investigation and constitute promising areas for future research.

In summary, this study highlights the potential impact of the BER pathway on several aspects of physiology, including lifespan, health span and neuronal survival in early stages of life. Moreover, it also uncovers the detrimental effects of DNA repair intermediates accumulation, resulting from incomplete and/or inefficient BER function, which contribute to AD pathophysiology (Figure 12). Deficiency of DNA glycosylases, which are essential for the initiation of BER, prevent the build-up of DNA repair intermediates leading to improvements in tau-dependent pathological features. Consequently, our study suggests that DNA glycosylases not only preserve genome integrity by repairing base lesions, but also modulate the transcriptional response of genes, by methylation and epigenetic regulation, to stress induced by tau-aggregation. Hence, the precise regulation and fine-tuning of DNA repair pathways have a critical role in promoting healthy aging and limiting the progression of AD.

Data availability

The accession number for the raw and processed RNA sequencing data reported in this paper is GEO: GSE235015. The code is available in the supplementary material.

Supplementary data

Supplementary Data are available at NAR Online.

Acknowledgements

The authors would like to thank Caleb Elwell for this support in this study. We thank Brian D. Ackley for sharing the EVL1372 strain. Some nematode strains used in this work were provided by the Caenorhabditis Genetics Center, which is funded by the NIH Office of Research Infrastructure Programs (P40 OD010440). Views and opinions expressed are however those of the author(s) only and do not necessarily reflect those of the European Union or the European Research Council. Neither the European Union nor the granting authority can be held responsible for them.

Funding

National Institute on Aging [AG000723, AG000578]; K.P. was supported by grants from the Fondation Santé [19656] Greece 2.0; National Recovery and Resilience Plan Flagship program TAEDR-0535850; European Research Council [GA 101077374 – SynaptoMitophagy]. Funding for open access charge: NIH.

Conflict of interest statement

None declared.

References

1. Graff-Radford,J., Yong,K.X.X., Apostolova,L.G., Bouwman,F.H., Carrillo,M., Dickerson,B.C., Rabinovici,G.D., Schott,J.M., Jones,D.T. and Murray,M.E. (2021) New insights into atypical Alzheimer's disease in the era of biomarkers. *Lancet Neurol.*, **20**, 222–234.
2. Ionescu-Tucker,A. and Cotman,C.W. (2021) Emerging roles of oxidative stress in brain aging and Alzheimer's disease. *Neurobiol. Aging*, **107**, 86–95.
3. Wilson,D.M. 3rd, Cookson,M.R., Van Den Bosch,L., Zetterberg,H., Holtzman,D.M. and Dewachter,I. (2023) Hallmarks of neurodegenerative diseases. *Cell*, **186**, 693–714.
4. de Sousa,M.M.L., Ye,J., Luna,L., Hildrestrand,G., Bjørås,K., Scheffler,K. and Bjørås,M. (2021) Impact of oxidative DNA damage and the role of DNA glycosylases in neurological dysfunction. *Int. J. Mol. Sci.*, **22**, 12924.
5. Dileep,V., Boix,C.A., Mathys,H., Marco,A., Welch,G.M., Meharena,H.S., Loon,A., Jeloka,R., Peng,Z., Bennett,D.A., *et al.* (2023) Neuronal DNA double-strand breaks lead to genome structural variations and 3D genome disruption in neurodegeneration. *Cell*, **186**, 4404–4421.
6. Caldecott,K.W. (2020) Mammalian DNA base excision repair: dancing in the moonlight. *DNA Repair (Amst.)*, **93**, 102921.
7. Weissman,L., Jo,D.G., Sørensen,M.M., de Souza-Pinto,N.C., Markesbery,W.R., Mattson,M.P. and Bohr,V.A. (2007) Defective DNA base excision repair in brain from individuals with Alzheimer's disease and amnestic mild cognitive impairment. *Nucleic Acids Res.*, **35**, 5545–5555.
8. Jacob,K.D., Noren Hooten,N., Tadokoro,T., Lohani,A., Barnes,J. and Evans,M.K. (2013) Alzheimer's disease-associated polymorphisms in human OGG1 alter catalytic activity and sensitize cells to DNA damage. *Free Radic. Biol. Med.*, **63**, 115–125.
9. Ertuzun,T., Semerci,A., Cakir,M.E., Ekmekcioglu,A., Gok,M.O., Soltys,D.T., de Souza-Pinto,N.C., Sezerman,U. and Muftuoglu,M. (2019) Investigation of base excision repair gene variants in late-onset Alzheimer's disease. *PLoS One*, **14**, e0221362.
10. Sykora,P., Misiak,M., Wang,Y., Ghosh,S., Leandro,G.S., Liu,D., Tian,J., Baptiste,B.A., Cong,W.N., Brenerman,B.M., *et al.* (2015) DNA polymerase β deficiency leads to neurodegeneration and exacerbates Alzheimer disease phenotypes. *Nucleic Acids Res.*, **43**, 943–959.
11. Calvo,J.A., Moroski-Erkul,C.A., Lake,A., Eichinger,L.W., Shah,D., Jhun,I., Limsirichai,P., Bronson,R.T., Christiani,D.C., Meira,L.B., *et al.* (2013) Aag DNA glycosylase promotes alkylation-induced tissue damage mediated by Parp1. *PLoS Genet.*, **9**, e1003413.
12. SenGupta,T., Palikaras,K., Esbensen,Y.Q., Konstantinidis,G., Galindo,F.J.N., Achanta,K., Kassahun,H., Stavgiannoudaki,I., Bohr,V.A., Akbari,M., *et al.* (2021) Base excision repair causes age-dependent accumulation of single-stranded DNA breaks that contribute to Parkinson disease pathology. *Cell Rep.*, **36**, 109668.
13. Lopes,A.F.C., Bozek,K., Herholz,M., Trifunovic,A., Rieckher,M. and Schumacher,B. (2020) A C. elegans model for neurodegeneration in Cockayne syndrome. *Nucleic Acids Res.*, **48**, 10973–10985.
14. Wilson,D.M., Rieckher,M., Williams,A.B. and Schumacher,B. (2017) Systematic analysis of DNA crosslink repair pathways during development and aging in Caenorhabditis elegans. *Nucleic Acids Res.*, **45**, 9467–9480.
15. Alvarez,J., Alvarez-Illera,P., Santo-Domingo,J., Fonteriz,R.I. and Montero,M. (2022) Modeling Alzheimer's disease in Caenorhabditis elegans. *Biomedicines*, **10**, 288.
16. Morinaga,H., Yonekura,S., Nakamura,N., Sugiyama,H., Yonei,S. and Zhang-Akiyama,Q.M. (2009) Purification and characterization of Caenorhabditis elegans NTH, a homolog of human endonuclease III: essential role of N-terminal region. *DNA Repair (Amst.)*, **8**, 844–851.
17. Hunter,S.E., Gustafson,M.A., Margillo,K.M., Lee,S.A., Ryde,I.T. and Meyer,J.N. (2012) In vivo repair of alkylating and oxidative

DNA damage in the mitochondrial and nuclear genomes of wild-type and glycosylase-deficient Caenorhabditis elegans. *DNA Repair (Amst.)*, **11**, 857–863.
18. Kassahun,H., SenGupta,T., Schiavi,A., Maglioni,S., Skjeldam,H.K., Arczewska,K., Brockway,N.L., Estes,S., Eide,L., Ventura,N., *et al.* (2018) Constitutive MAP-kinase activation suppresses germline apoptosis in NTH-1 DNA glycosylase deficient C. elegans. *DNA Repair (Amst.)*, **61**, 46–55.
19. Palikaras,K., Lionaki,E. and Tavernarakis,N. (2015) Coordination of mitophagy and mitochondrial biogenesis during ageing in C. elegans. *Nature*, **521**, 525–528.
20. Fang,E.F., Kassahun,H., Croteau,D.L., Scheibye-Knudsen,M., Marosi,K., Lu,H., Shamanna,R.A., Kalyanasundaram,S., Bollineni,R.C., Wilson,M.A., *et al.* (2016) NAD(+) replenishment improves lifespan and healthspan in Ataxia Telangiectasia models via mitophagy and DNA repair. *Cell Metab.*, **24**, 566–581.
21. Henze,A., Homann,T., Rohn,I., Aschner,M., Link,C.D., Kleuser,B., Schweigert,F.J., Schwerdtle,T. and Bornhorst,J. (2016) Caenorhabditis elegans as a model system to study post-translational modifications of human transthyretin. *Sci. Rep.*, **6**, 37346.
22. García-Rodríguez,F.J., Martínez-Fernández,C., Brena,D., Kukhtar,D., Serrat,X., Nadal,E., Boxem,M., Honnen,S., Miranda-Vizuete,A., Villanueva,A., *et al.* (2018) Genetic and cellular sensitivity of Caenorhabditis elegans to the chemotherapeutic agent cisplatin. *Dis. Model Mech.*, **11**, dmm033506.
23. Mortazavi,A., Williams,B.A., McCue,K., Schaeffer,L. and Wold,B. (2008) Mapping and quantifying mammalian transcriptomes by RNA-seq. *Nat. Methods*, **5**, 621–628.
24. Angeles-Albores,D., RY,N.L., Chan,J. and Sternberg,P.W. (2016) Tissue enrichment analysis for C. elegans genomics. *BMC Bioinf.*, **17**, 366.
25. Angeles-Albores,D., Lee,R., Chan,J. and Sternberg,P. (2018) Two new functions in the WormBase Enrichment Suite. *MicroPubl Biol.*, **2018**, 10.17912/W25Q2N.
26. Grubman,A., Chew,G., Ouyang,J.F., Sun,G., Choo,X.Y., McLean,C., Simmons,R.K., Buckberry,S., Vargas-Landin,D.B., Poppe,D., *et al.* (2019) A single-cell atlas of entorhinal cortex from individuals with Alzheimer's disease reveals cell-type-specific gene expression regulation. *Nat. Neurosci.*, **22**, 2087–2097.
27. Ali,M., Huarte,O.U., Heurtaux,T., Garcia,P., Rodriguez,B.P., Grzyb,K., Halder,R., Skupin,A., Buttini,M. and Glaab,E. (2024) Single-cell transcriptional profiling and gene regulatory network modeling in Tg2576 mice reveal gender-dependent molecular features preceding Alzheimer-like pathologies. *Mol. Neurobiol.*, **61**, 541–566.
28. Shaw,L.M., Vanderstichele,H., Knapik-Czajka,M., Clark,C.M., Aisen,P.S., Petersen,R.C., Blennow,K., Soares,H., Simon,A., Lewczuk,P., *et al.* (2009) Cerebrospinal fluid biomarker signature in Alzheimer's disease neuroimaging initiative subjects. *Ann. Neurol.*, **65**, 403–413.
29. Dang,M., Chen,Q., Zhao,X., Chen,K., Li,X., Zhang,J., Lu,J., Ai,L., Chen,Y. and Zhang,Z. (2023) Tau as a biomarker of cognitive impairment and neuropsychiatric symptom in Alzheimer's disease. *Hum. Brain Mapp.*, **44**, 327–340.
30. Fatouros,C., Pir,G.J., Biernat,J., Koushika,S.P., Mandelkow,E., Mandelkow,E.M., Schmidt,E. and Baumeister,R. (2012) Inhibition of tau aggregation in a novel Caenorhabditis elegans model of tauopathy mitigates proteotoxicity. *Hum. Mol. Genet.*, **21**, 3587–3603.
31. Fang,E.F., Hou,Y., Palikaras,K., Adriaanse,B.A., Kerr,J.S., Yang,B., Lautrup,S., Hasan-Olive,M.M., Caponio,D., Dan,X., *et al.* (2019) Mitophagy inhibits amyloid-β and tau pathology and reverses cognitive deficits in models of Alzheimer's disease. *Nat. Neurosci.*, **22**, 401–412.
32. Tarawneh,R. and Holtzman,D.M. (2012) The clinical problem of symptomatic Alzheimer disease and mild cognitive impairment. *Cold Spring Harb. Perspect. Med.*, **2**, a006148.
33. Murphy,C. (2019) Olfactory and other sensory impairments in Alzheimer disease. *Nat. Rev. Neurol.*, **15**, 11–24.
34. Dan,X., Wechter,N., Gray,S., Mohanty,J.G., Croteau,D.L. and Bohr,V.A. (2021) Olfactory dysfunction in aging and neurodegenerative diseases. *Ageing Res. Rev.*, **70**, 101416.
35. Cao,S.Q., Wang,H.L., Palikaras,K., Tavernarakis,N. and Fang,E.F. (2023) Chemotaxis assay for evaluation of memory-like behavior in wild-type and Alzheimer's-disease-like C. elegans models. *STAR Protoc*, **4**, 102250.
36. Aquino Nunez,W., Combs,B., Gamblin,T.C. and Ackley,B.D. (2022) Age-dependent accumulation of tau aggregation in Caenorhabditis elegans. *Front Aging*, **3**, 928574.
37. Fong,S., Teo,E., Ng,L.F., Chen,C.B., Lakshmanan,L.N., Tsoi,S.Y., Moore,P.K., Inoue,T., Halliwell,B. and Gruber,J. (2016) Energy crisis precedes global metabolic failure in a novel Caenorhabditis elegans Alzheimer disease model. *Sci. Rep.*, **6**, 33781.
38. Begcevic,I., Brinc,D., Brown,M., Martinez-Morillo,E., Goldhardt,O., Grimmer,T., Magdolen,V., Batruch,I. and Diamandis,E.P. (2018) Brain-related proteins as potential CSF biomarkers of Alzheimer's disease: a targeted mass spectrometry approach. *J. Proteomics*, **182**, 12–20.
39. Fensgård,Ø., Kassahun,H., Bombik,I., Rognes,T., Lindvall,J.M. and Nilsen,H. (2010) A two-tiered compensatory response to loss of DNA repair modulates aging and stress response pathways. *Aging (Albany NY)*, **2**, 133–159.
40. Muftuoglu,M., de Souza-Pinto,N.C., Dogan,A., Aamann,M., Stevnsner,T., Rybanska,I., Kirkali,G., Dizdaroglu,M. and Bohr,V.A. (2009) Cockayne syndrome group B protein stimulates repair of formamidopyrimidines by NEIL1 DNA glycosylase. *J. Biol. Chem.*, **284**, 9270–9279.
41. Elsakrmy,N., Zhang-Akiyama,Q.M. and Ramotar,D. (2020) The base excision repair pathway in the Nematode Caenorhabditis elegans. *Front. Cell Dev. Biol.*, **8**, 598860.
42. Tiwari,V. and Wilson,D.M. 3rd (2019) DNA damage and associated DNA repair defects in disease and premature aging. *Am. J. Hum. Genet.*, **105**, 237–257.
43. Kerr,J.S., Adriaanse,B.A., Greig,N.H., Mattson,M.P., Cader,M.Z., Bohr,V.A. and Fang,E.F. (2017) Mitophagy and Alzheimer's disease: cellular and molecular mechanisms. *Trends Neurosci.*, **40**, 151–166.
44. Sarasija,S. and Norman,K.R. (2018) Analysis of mitochondrial structure in the body wall muscle of Caenorhabditis elegans. *Bio Protoc.*, **8**, e2801.
45. Hou,Y., Dan,X., Babbar,M., Wei,Y., Hasselbalch,S.G., Croteau,D.L. and Bohr,V.A. (2019) Ageing as a risk factor for neurodegenerative disease. *Nat. Rev. Neurol.*, **15**, 565–581.
46. Milano,L., Charlier,C.F., Andreguetti,R., Cox,T., Healing,E., Thomé,M.P., Elliott,R.M., Samson,L.D., Masson,J.Y., Lenz,G., *et al.* (2022) A DNA repair-independent role for alkyladenine DNA glycosylase in alkylation-induced unfolded protein response. *Proc. Natl. Acad. Sci. U.S.A.*, **119**, e2111404119.
47. Hao,W., Wang,J., Zhang,Y., Wang,C., Xia,L., Zhang,W., Zafar,M., Kang,J.Y., Wang,R., Ali Bohio,A., *et al.* (2020) Enzymatically inactive OGG1 binds to DNA and steers base excision repair toward gene transcription. *FASEB J.*, **34**, 7427–7441.
48. Ewald,C.Y. and Li,C. (2010) Understanding the molecular basis of Alzheimer's disease using a Caenorhabditis elegans model system. *Brain Struct Funct*, **214**, 263–283.
49. Kraemer,B.C., Zhang,B., Leverenz,J.B., Thomas,J.H., Trojanowski,J.Q. and Schellenberg,G.D. (2003) Neurodegeneration and defective neurotransmission in a Caenorhabditis elegans model of tauopathy. *Proc. Natl. Acad. Sci. U.S.A.*, **100**, 9980–9985.
50. Miyasaka,T., Ding,Z., Gengyo-Ando,K., Oue,M., Yamaguchi,H., Mitani,S. and Ihara,Y. (2005) Progressive neurodegeneration in C. elegans model of tauopathy. *Neurobiol. Dis.*, **20**, 372–383.
51. Hornsten,A., Lieberthal,J., Fadia,S., Malins,R., Ha,L., Xu,X., Daigle,I., Markowitz,M., O'Connor,G., Plasterk,R., *et al.* (2007) APL-1, a Caenorhabditis elegans protein related to the human

beta-amyloid precursor protein, is essential for viability. *Proc. Natl. Acad. Sci. U.S.A.*, **104**, 1971–1976.
52. Wang,J., Markesbery,W.R. and Lovell,M.A. (2006) Increased oxidative damage in nuclear and mitochondrial DNA in mild cognitive impairment. *J. Neurochem.*, **96**, 825–832.
53. Jones,S.K., Nee,L.E., Sweet,L., Polinsky,R.J., Bartlett,J.D., Bradley,W.G. and Robison,S.H. (1989) Decreased DNA repair in familial Alzheimer's disease. *Mutat. Res.*, **219**, 247–255.
54. Iida,T., Furuta,A., Nishioka,K., Nakabeppu,Y. and Iwaki,T. (2002) Expression of 8-oxoguanine DNA glycosylase is reduced and associated with neurofibrillary tangles in Alzheimer's disease brain. *Acta Neuropathol.*, **103**, 20–25.
55. Jacobsen,E., Beach,T., Shen,Y., Li,R. and Chang,Y. (2004) Deficiency of the Mre11 DNA repair complex in Alzheimer's disease brains. *Brain Res. Mol. Brain Res.*, **128**, 1–7.
56. Weissman,L., de Souza-Pinto,N.C., Mattson,M.P. and Bohr,V.A. (2009) DNA base excision repair activities in mouse models of Alzheimer's disease. *Neurobiol. Aging*, **30**, 2080–2081.
57. Lillenes,M.S., Rabano,A., Støen,M., Riaz,T., Misaghian,D., Møllersen,L., Esbensen,Y., Günther,C.C., Selnes,P., Stenset,V.T., *et al.* (2016) Altered DNA base excision repair profile in brain tissue and blood in Alzheimer's disease. *Mol. Brain*, **9**, 61.
58. Misiak,M., Vergara Greeno,R., Baptiste,B.A., Sykora,P., Liu,D., Cordonnier,S., Fang,E.F., Croteau,D.L., Mattson,M.P. and Bohr,V.A. (2017) DNA polymerase β decrement triggers death of olfactory bulb cells and impairs olfaction in a mouse model of Alzheimer's disease. *Aging Cell*, **16**, 162–172.
59. Will,C.L. and Lührmann,R. (2011) Spliceosome structure and function. *Cold Spring Harb. Perspect. Biol.*, **3**, a003707.
60. Raj,T., Li,Y.I., Wong,G., Humphrey,J., Wang,M., Ramdhani,S., Wang,Y.C., Ng,B., Gupta,I., Haroutunian,V., *et al.* (2018) Integrative transcriptome analyses of the aging brain implicate altered splicing in Alzheimer's disease susceptibility. *Nat. Genet.*, **50**, 1584–1592.
61. Hsieh,Y.C., Guo,C., Yalamanchili,H.K., Abreha,M., Al-Ouran,R., Li,Y., Dammer,E.B., Lah,J.J., Levey,A.I., Bennett,D.A., *et al.* (2019) Tau-mediated disruption of the spliceosome triggers cryptic RNA splicing and neurodegeneration in Alzheimer's disease. *Cell Rep.*, **29**, 301–316.
62. Bai,B., Hales,C.M., Chen,P.C., Gozal,Y., Dammer,E.B., Fritz,J.J., Wang,X., Xia,Q., Duong,D.M., Street,C., *et al.* (2013) U1 small nuclear ribonucleoprotein complex and RNA splicing alterations in Alzheimer's disease. *Proc. Natl. Acad. Sci. U.S.A.*, **110**, 16562–16567.
63. Rockenstein,E.M., McConlogue,L., Tan,H., Power,M., Masliah,E. and Mucke,L. (1995) Levels and alternative splicing of amyloid beta protein precursor (APP) transcripts in brains of APP transgenic mice and humans with Alzheimer's disease. *J. Biol. Chem.*, **270**, 28257–28267.
64. Buée,L., Bussière,T., Buée-Scherrer,V., Delacourte,A. and Hof,P.R. (2000) Tau protein isoforms, phosphorylation and role in neurodegenerative disorders. *Brain Res. Brain Res. Rev.*, **33**, 95–130.
65. Arribere,J.A., Kuroyanagi,H. and Hundley,H.A. (2020) mRNA editing, processing and quality control in Caenorhabditis elegans. *Genetics*, **215**, 531–568.
66. Nikolaidis,N. and Nei,M. (2004) Concerted and nonconcerted evolution of the Hsp70 gene superfamily in two sibling species of nematodes. *Mol. Biol. Evol.*, **21**, 498–505.
67. Snutch,T.P. and Baillie,D.L. (1984) A high degree of DNA strain polymorphism associated with the major heat shock gene in Caenorhabditis elegans. *Mol. Gen. Genet.*, **195**, 329–335.
68. Morley,J.F. and Morimoto,R.I. (2004) Regulation of longevity in Caenorhabditis elegans by heat shock factor and molecular chaperones. *Mol. Biol. Cell*, **15**, 657–664.
69. Nollen,E.A., Garcia,S.M., van Haaften,G., Kim,S., Chavez,A., Morimoto,R.I. and Plasterk,R.H. (2004) Genome-wide RNA interference screen identifies previously undescribed regulators of polyglutamine aggregation. *Proc. Natl. Acad. Sci. U.S.A.*, **101**, 6403–6408.

Received: June 22, 2023. **Revised:** July 20, 2024. **Editorial Decision:** July 26, 2024. **Accepted:** August 11, 2024
Published by Oxford University Press on behalf of Nucleic Acids Research 2024.